Adjunct

Mathematical Description of the VLIDORT RT model

This adjunct document contains the mathematical description of the VLIDORT RT model, including the supplements. There are five main sections. The first and largest section presents the general discrete-ordinate solution of the Stokes 4-vector radiative transfer equation (RTE), with the particular integral determination based on classical substitution methods; this section also includes solution of the multi-layer boundary value problem and the determination of "post-processed" radiation fields through source function integration. Mathematical descriptions of all aspects of the linearization process (that is, analytic differentiation with respect to atmospheric and surface optical properties) are given at each stage of the complete solution for the radiation-field solution.

The second section deals explicitly with ancillary numerical techniques used in VLIDORT to deal with certain performance enhancements and computational issues. In some cases, this section expands on summary material given in the main guide. The third and fourth sections give mathematical details of the VBRDF kernels used in the VLIDORT's VBRDF supplement and ocean optics related to water surface-leaving radiances in the VSLEAVE supplement, respectively. References given in this adjunct are listed at the end.

Table of Contents

A1. Description of the VLIDORT Model

A1.1 RTE Solution Strategy

In the VLIDORT main guide, we give a more theoretical description for solving the RTE in vector form. Here, we go into the details of solving not only both the basic equation, but also descriptions of the linearization process for generating analytic weighting functions.

The solution strategy has two stages. In the first step, for each layer, we establish discrete ordinate solutions to the homogeneous RTE in the absence of sources (section A1.2.1). In sections A1.2.3 and A1.2.4, we use exponential-substitution methods to solve for particular integrals of the RTE with solar scattering and thermal emission source terms, respectively. In the second stage, application of the boundary conditions leads to a complete solution of the discrete ordinate radiation field in the whole atmosphere, and we finish the solution by deploying source function integration of the RTE in order to establish solutions away from discrete ordinate directions (section A1.3).

Additional implementations are discussed in sections A1.4 through A1.6. These include the more exact treatments of single scatter in spherical geometry (section A1.4) and the treatment of total atmospheric column and blackbody weighting functions (sections A1.5 and A1.6).

The complete vector RT solution for a plane-parallel single-layer slab was developed by Siewert [*Siewert*, 2000], and we follow some elements in this formulation. Our description also adheres closely to the LIDORT treatment, especially concerning the construction and solution of the boundary-value problem and the linearization methodology.

In the following sections, we suppress the Fourier index m unless noted explicitly, and wavelength dependence is implicit throughout. We sometimes suppress the layer index n in the interests of clarity. All matrices are written in bold typeface, with careful distinction made between 4x4 matrices and 4-vectors and $4N_d$ x $4N_d$ matrices and $4N_d$-vectors, where N_d is the number of discrete ordinate directions in the half-space.

A1.2 Discrete Ordinate Solutions and Linearizations

A1.2.1 Homogeneous RTE, Eigenproblem reduction

First, we solve Eq. (A1.1.24) without the solar source term. For each Fourier term m, the multiple scatter integral over the upper and lower polar direction half-spaces is approximated by a double Gaussian quadrature scheme [*Thomas and Stamnes*, 1999], with stream directions $\{\pm\mu_i\}$ and Gauss-Legendre weights $\{c_i\}$ for $i = 1, \ldots N_d$, where N_d is the number of discrete ordinates in the polar half space. The resulting vector RTE in layer n, for Fourier component m is then

$$\pm\mu_i \frac{d\mathbf{I}_m(x,\pm\mu_i)}{dx} \pm \mathbf{I}_m(x,\pm\mu_i) = \frac{\omega}{2}\sum_{l=m}^{M} \mathbf{P}_l^m(\pm\mu_i)\mathbf{B}_l \sum_{j=1}^{N_d}\left[\mathbf{P}_l^m(\mu_j)\mathbf{I}_m(x,\mu_j) + \mathbf{P}_l^m(-\mu_j)\mathbf{I}_m(x,-\mu_j)\right]. \quad \text{(A1.2.1)}$$

There are $8N_d$ coupled first-order linear differential equations for $\mathbf{I}_m(x,\pm\mu_i)$ in this system, which is solved by eigenvalue methods [*Thomas and Stamnes*, 1999; *Siewert*, 2000], using the *ansatz*:

$$\mathbf{I}_\alpha(x,\pm\mu_i) = \mathbf{W}_\alpha(\pm\mu_i)\exp[-k_\alpha x]. \tag{A1.2.2}$$

We then define the following two vectors of rank $4N_d$:

$$\mathbb{W}_\alpha^{\pm} = \left[\mathbf{W}_\alpha^{\mathrm{T}}(\pm\mu_1), \mathbf{W}_\alpha^{\mathrm{T}}(\pm\mu_2), \ldots, \mathbf{W}_\alpha^{\mathrm{T}}\left(\pm\mu_{N_d}\right)\right]^{\mathrm{T}}. \tag{A1.2.3}$$

The system is decoupled using sum and difference vectors $\mathbb{X}_\alpha = \mathbb{W}_\alpha^{+} + \mathbb{W}_\alpha^{-}$ and $\mathbb{Y}_\alpha = \mathbb{W}_\alpha^{+} - \mathbb{W}_\alpha^{-}$, and the order is then be reduced from $8N_d$ to $4N_d$. The result is an eigenproblem for the collection of separation constants and associated solution vectors $\{k_\alpha, \mathbb{X}_\alpha\}$, where index $\alpha = 1, \ldots, 4N_d$ labels the eigensolutions. The eigenmatrix for this system is constructed from the optical property inputs $\{\omega, \mathbf{B}_l\}$ and combination products of matrices $\mathbf{P}_l^m(\pm\mu_i)$. The eigenproblem is [*Siewert*, 2000]:

$$\mathbb{X}_\alpha^{*}\mathbb{G} = k_\alpha^2\mathbb{X}_\alpha^{*};\ \ \mathbb{G}\mathbb{X}_\alpha = k_\alpha^2\mathbb{X}_\alpha; \tag{A1.2.4}$$

$$\mathbb{G} = \mathbb{F}^{+}\mathbb{F}^{-};\ \ \mathbb{F}^{\pm} = \left[\mathbb{E} - \frac{\omega}{2}\sum_{l=m}^{M}\mathbb{P}(l,m)\mathbf{B}_l\mathbf{A}^{\pm}\mathbb{P}^{\mathrm{T}}(l,m)\,\mathbb{C}\right]\mathbb{M}^{-1}; \tag{A1.2.5}$$

$$\mathbb{P}(l,m) = Diag[\mathbf{P}_l^m(\mu_1), \mathbf{P}_l^m(\mu_2), \ldots, \mathbf{P}_l^m\left(\mu_{N_d}\right)]^{\mathrm{T}}; \tag{A1.2.6}$$

$$\mathbb{M} = Diag\left[\mu_1\mathbf{E}, \mu_2\mathbf{E}, \ldots, \mu_{N_d}\mathbf{E}\right];\ \mathbb{C} = Diag\left[c_1\mathbf{E}, c_2\mathbf{E}, \ldots, c_{N_d}\mathbf{E}\right]. \tag{A1.2.7}$$

Here, $\mathbf{A}^{\pm} = \mathbf{E} \pm (-1)^{l-m}\mathbf{D}$; $\mathbf{E} = Diag[1,1,1,1]$; $\mathbf{D} = Diag[1,1,-1,-1]$, $\mathbb{E}$ is the $4N_d$ x $4N_d$ identity matrix; $\mathbb{X}_\alpha^{*}$ and $\mathbb{X}_\alpha$ are the left and right eigenvectors respectively, with $\mathbb{X}_\alpha^{*}$ the conjugate transpose of $\mathbb{X}_\alpha$. Vectors $\mathbb{X}_\alpha$ and $\mathbb{W}_\alpha^{\pm}$ are connected through the auxiliary equations:

$$\mathbb{W}_\alpha^{\pm} = \frac{1}{2}\mathbb{M}^{-1}\left[\mathbb{E} \pm \frac{1}{k_\alpha}\mathbb{F}^{+}\right]\mathbb{X}_\alpha. \tag{A1.2.8}$$

Eigenvalues occur in pairs $\{\pm k_\alpha\}$. Left and right eigenvectors share the same spectrum of eigenvalues. As noted by [*Siewert*, 2000], both complex- and real-variable eigensolutions may be present in the full Stokes 4-vector case (rank $4N_d$). Eigensolutions may be determined numerically with the complex-variable eigensolver DGEEV from the LAPACK suite [*Anderson et al*., 1995]. DGEEV generates both right and left eigenvectors, which have unit moduli.

DGEEV must be used for Stokes 4-vector calculations for an atmosphere with scattering by aerosols or clouds, since there will be complex eigensolutions in this case. However, for the scalar case (no polarization, solutions only for the I-component of the Stokes vector), or the Stokes 3-vector case for $\{I, Q, U\}$, the eigenmatrix $\mathbb{G}$ is symmetric and all eigensolutions are real-valued. In this case, the ASYMTX [*Stamnes et al*., 1988] eigensolver (which is really an adaptation of DGEEV for real-valued eigenproblems) may be used; unlike DGEEV it delivers only the right eigenvectors. Linearization of the homogeneous solutions from DGEEV uses adjoint theory and has some subtleties; adjoint solutions are not available for ASYMTX. We deal with this in the next section.

The symmetry of ASYMTX arises from the following considerations. It turns out that, aside from additional elements down the diagonal, the eigenmatrix $\mathbb{G}$ in Eqn. (A1.2.4) consists of blocks of 4x4 matrices of the form $\mathbf{P}_{lm}(\mu_i)\mathbf{B}_l\mathbf{P}_{lm}^{\mathrm{T}}(\mu_j)$, Since $\mathbf{P}$ and $\mathbf{P}^{\mathrm{T}}$ are symmetric, then $\mathbb{G}$ will be symmetric if $\mathbf{B}_l$ is also symmetric. In other words, $\mathbb{G}$ will be symmetric if the Greek constants ε_l in $\mathbf{B}_l$ are zero for all values of l.

The policy in VLIDORT is be to retain both eigensolvers and use them as appropriate – if any of the Greek constants ε_l in $\mathbf{B}_l$ is non-zero for a given scattering layer, then the complex eigensolver DGEEV is selected for that layer; otherwise, we use ASYMTX. For Stokes 4-vector computations with a few aerosol/cloud layers in an otherwise Rayleigh-scattering atmosphere, both eigensolvers will be required. Circular polarization in the Earth's atmosphere is typically three orders of magnitude smaller that its linear counterpart; it is often neglected in RT simulations. For a 3-component calculation of $\{I, Q, U\}$, VLIDORT uses 3x3 Mueller and scattering matrices, and the use of ASYMTX in these situations will provide considerable savings in CPU time (it is approximately twice as fast as DGEEV).

Returning to the full Stokes 4-vector case, the complete homogeneous solution in one layer is then:

$$\mathbb{I}^+(x) = \mathbb{D}^+ \sum_{\alpha=1}^{4N_d} \{\mathfrak{L}_\alpha \mathbb{W}_\alpha^+ \exp[-k_\alpha x] + \mathfrak{M}_\alpha \mathbb{W}_\alpha^- \exp[-k_\alpha(\Delta - x)]\}; \qquad \text{(A1.2.9)}$$

$$\mathbb{I}^-(x) = \mathbb{D}^- \sum_{\alpha=1}^{4N_d} \{\mathfrak{L}_\alpha \mathbb{W}_\alpha^- \exp[-k_\alpha x] + \mathfrak{M}_\alpha \mathbb{W}_\alpha^+ \exp[-k_\alpha(\Delta - x)]\}; \qquad \text{(A1.2.10)}$$

Here, $\mathbb{D}^- = Diag[\mathbf{D}, \mathbf{D}, \ldots \mathbf{D}]$, and $\mathbb{D}^+ = \mathbb{E}$; these matrices arise from application of symmetry relations [*Siewert*, 2000]. The use of optical thickness $\Delta - x$ in the second exponential ensures that solutions remain bounded [*Stamnes and Conklin*, 1984]. The quantities $\{\mathfrak{L}_\alpha, \mathfrak{M}_\alpha\}$ are the constants of integration; determined by application of the boundary conditions and solution of the resulting boundary-value problem.

In the Stokes 4-vector case, some contributions to $\mathbb{I}^\pm(x)$ will be complex, some real. It is understood that we compute the real parts of any complex variable expressions. Thus for example if $\{k_\alpha, \mathbb{W}_\alpha^-\}$ is a complex eigensolution with associated (complex) integration constant $\mathfrak{L}_\alpha$, the real part of the solution will be:

$$\mathrm{Re}[\mathfrak{L}_\alpha \mathbb{W}_\alpha^- e^{-k_\alpha x}] = \mathrm{Re}[\mathfrak{L}_\alpha]\mathrm{Re}[\mathbb{W}_\alpha^- e^{-k_\alpha x}] - \mathrm{Im}[\mathfrak{L}_\alpha]\mathrm{Im}[\mathbb{W}_\alpha^- e^{-k_\alpha x}]. \qquad \text{(A1.2.11)}$$

From a bookkeeping standpoint, one must keep count of the number of real and complex solutions, and treat them separately in the numerical implementation. In the interests of clarity, we have not made an explicit separation of complex variables, and it will be clear from the context whether real or complex variables are under consideration.

A1.2.2 Linearization of the eigenproblem

We require derivatives of the above eigensolutions with respect to some *atmospheric* variable ξ in layer n. In this section, the layering index is suppressed for ease of exposition. . The starting point for the differentiation is the set of linearized optical properties $\mathcal{V} \equiv \xi\, {}^{\partial\Delta}/_{\partial\xi}$; $\mathcal{U} \equiv \xi\, {}^{\partial\omega}/_{\partial\xi}$; $\mathcal{Z}_l \equiv \xi\, {}^{\partial\mathbf{B}_l}/_{\partial\xi}$, that is, normalized partial derivatives of the set of IOPs $\{\Delta, \omega, \mathbf{B}_l\}$. Here, the eigensolutions $\{k_\alpha, \mathbf{X}_\alpha^\pm\}$ depend only on the quantities $\{\omega, \mathbf{B}_l\}$. Applying the linearization operator $\mathcal{L} \equiv \xi\, {}^{\partial}/_{\partial\xi}$ to the eigenmatrix $\mathbf{\Gamma}$, we find

$$\mathcal{L}(\mathbb{G}) = \mathcal{L}(\mathbb{F}^+)\mathbb{F}^- + \mathbb{F}^+\mathcal{L}(\mathbb{F}^-); \qquad \text{(A1.2.12)}$$

$$\mathcal{L}(\mathbb{F}^\pm) = -\left[\frac{1}{2}\{\mathcal{U}\mathbb{P}_{lm}\mathbf{B}_l + \omega\mathbb{P}_{lm}\mathcal{Z}_l\}\mathbf{A}^\pm\mathbb{P}_{lm}^{\mathrm{T}}\mathbb{C}\right]\mathbb{M}^{-1}. \qquad \text{(A1.2.13)}$$

Linearization treatments are different for the full Stokes 4-vector case, and the scalar and Stokes 3-vector situations.

4-vector case. We apply linearization to both the left and right eigensystems:

$$\mathcal{L}(\mathbb{X}_\alpha^*)\mathbb{G} + \mathbb{X}_\alpha^*\mathcal{L}(\mathbb{G}) = 2k_\alpha\mathcal{L}(k_\alpha)\mathbb{X}_\alpha^* + k_\alpha^2\mathcal{L}(\mathbb{X}_\alpha^*); \tag{A1.2.14}$$

$$\mathbb{G}\mathcal{L}(\mathbb{X}_\alpha) + \mathcal{L}(\mathbb{G})\mathbb{X}_\alpha = 2k_\alpha\mathcal{L}(k_\alpha)\mathbb{X}_\alpha + k_\alpha^2\mathcal{L}(\mathbb{X}_\alpha). \tag{A1.2.15}$$

We form a dot product $\otimes$ by pre-multiplying the second of these equations by the transpose vector $\mathbb{X}_\alpha^*$:

$$\mathbb{X}_\alpha^* \otimes \mathbb{G}\mathcal{L}(\mathbb{X}_\alpha) + \mathbb{X}_\alpha^* \otimes \mathcal{L}(\mathbb{G})\mathbb{X}_\alpha = 2k_\alpha\mathcal{L}(k_\alpha)\mathbb{X}_\alpha^* \otimes \mathbb{X}_\alpha + k_\alpha^2\mathbb{X}_\alpha^* \otimes \mathcal{L}(\mathbb{X}_\alpha). \tag{A1.2.16}$$

Using the relation $\mathbb{X}_\alpha^* \otimes \mathbb{G}\mathcal{L}(\mathbb{X}_\alpha) = \mathbb{X}_\alpha^*\mathbb{G} \otimes \mathcal{L}(\mathbb{X}_\alpha) = k_\alpha^2\mathbb{X}_\alpha^* \otimes \mathcal{L}(\mathbb{X}_\alpha)$, we find that

$$y_\alpha \equiv \mathcal{L}(k_\alpha) = \frac{\mathbb{X}_\alpha^* \otimes \mathcal{L}(\mathbb{G})\mathbb{X}_\alpha}{2k_\alpha\mathbb{X}_\alpha^* \otimes \mathbb{X}_\alpha}. \tag{A1.2.17}$$

This is the linearization of the separation constants. Next, we substitute this result in Eq. (A1.2.14) to obtain the following linear algebra problem for each eigensolution linearization:

$$\mathbb{H}_\alpha\mathcal{L}(\mathbb{X}_\alpha) = \mathbb{C}_\alpha; \qquad \mathbb{H}_\alpha = \mathbb{G} - k_\alpha^2\mathbb{E}; \qquad \mathbb{C}_\alpha = 2k_\alpha y_\alpha\mathbb{X}_\alpha - \mathcal{L}(\mathbb{G})\mathbb{X}_\alpha. \tag{A1.2.18}$$

For real eigensolutions, this system has rank $4N_d$, and for complex solutions, the rank is $8N_d$.

Implementation of this system of equations "as is" is not possible due to the degeneracy of the eigenproblem, and we need additional constraints to find the unique solution for $\mathcal{L}(\mathbb{X}_\alpha)$. The treatment for real and complex solutions is different.

For the real-valued eigensolutions, the unit-modulus eigenvector normalization is $\mathbb{X}_\alpha \otimes \mathbb{X}_\alpha = 1$ in dot-product notation. Linearizing, this yields one equation

$$\mathcal{L}(\mathbb{X}_\alpha) \otimes \mathbb{X}_\alpha + \mathbb{X}_\alpha \otimes \mathcal{L}(\mathbb{X}_\alpha) = 0. \tag{A1.2.19}$$

The solution procedure uses $4N_d - 1$ equations from Eq. (A1.2.18), along with Eq. (A1.2.19) to form a slightly modified linear system of rank $4N_d$. This system is then solved by standard means using the DGETRF and DGETRS LU-decomposition routines from the LAPACK suite.

For complex-valued eigensolutions, Eq. (A1.2.18) is a complex-variable system for both the real and imaginary parts of the linearized eigenvectors. There are $8N_d$ equations in all, but now we require two constraint conditions to remove the eigenproblem arbitrariness. The first is Eq. (A1.2.19). The second condition is imposed by the following normalization from the LAPACK DGEEV routine for solution of complex-valued eigenproblems: for that element of a (complex-valued) eigenvector which has the largest real value, the corresponding imaginary part is always set to zero. Thus, for eigenvector $\mathbb{X}_\alpha$ with components $\mathrm{X}_j \in \mathbb{X}_\alpha, j = 1,2,\ldots 4N_d$, if X_q satisfies condition $\mathrm{Re}[\mathrm{X}_q] = \max_{j=1,2,\ldots 4N_d}\{\mathrm{Re}[\mathrm{X}_j]\}$, then $\mathrm{Im}[\mathrm{X}_q] = 0$, and consequently $\mathcal{L}\big(\mathrm{Im}[\mathrm{X}_q]\big) = 0$. This is the second condition. The solution procedure is then: (1) in Eq. (A1.2.19) to strike out row q and column q in matrix $\mathbb{H}_\alpha$ for which $\mathrm{Im}[\mathrm{X}_q]$ is zero, then remove column q in vector $\mathbb{C}_\alpha$; and (2) in the resulting system of rank $8N_d - 1$, replace one of the rows with the normalization constraint Eq. (A1.2.19). $\mathcal{L}(\mathbb{X}_\alpha)$ is then the solution of the resulting linear system.

Scalar and 3-vector case. Here the (real-valued) eigensolutions are obtained using eigensolver ASYMTX – this has no adjoint solution, so there is no determination of $\mathcal{L}(k_\alpha)$ as in Eq. (A1.2.17). Instead, we solve for variables $\{\mathcal{L}(k_\alpha), \mathcal{L}(\mathbb{X}_\alpha)\}$ using $\mathbb{H}_\alpha\mathcal{L}(\mathbb{X}_\alpha) = 2k_\alpha\mathcal{L}(k_\alpha)\mathbb{X}_\alpha -$

$\mathcal{L}(\mathbb{G})\mathbb{X}_\alpha$ from above, plus the normalization condition to form a joint system of rank $3N_d + 1$ (vector) or rank $N_d + 1$ (scalar).

Having derived the linearizations $\{\mathcal{L}(k_\alpha), \mathcal{L}(\mathbb{X}_\alpha)\}$, we complete this section by differentiating the auxiliary result in Eq. (A1.2.11) to establish $\mathcal{L}(\mathbb{W}_\alpha^\pm)$:

$$\mathcal{L}(\mathbb{W}_\alpha^\pm) = \tfrac{1}{2}\mathbb{M}^{-1}\left[\mp\tfrac{\mathcal{L}(k_\alpha)}{k_\alpha^2}\mathbb{F}^+ \pm \tfrac{1}{k_\alpha}\mathcal{L}(\mathbb{F}^+)\right]\mathbb{X}_\alpha + \tfrac{1}{2}\mathbb{M}^{-1}\left[\mathbb{E} \pm \tfrac{1}{k_\alpha}\mathbb{F}^+\right]\mathcal{L}(\mathbb{X}_\alpha). \qquad \text{(A1.2.20)}$$

Finally, we have linearizations of the transmittance derivatives in Eq. (A1.2.12):

$$\mathcal{L}(\exp[-k_\alpha x]) = -[x\mathcal{L}(k_\alpha) + k_\alpha\mathcal{L}(x)]\exp[-k_\alpha x]. \qquad \text{(A1.2.21)}$$

Since the partial layer optical thickness x is proportional to the total layer optical depth Δ in an optically uniform layer, we have $\mathcal{L}(x) = {}^{x}/_{\Delta}\,\mathcal{L}(\Delta) = {}^{x}/_{\Delta}\,\mathcal{V}$ in terms of the basic linearized optical property input $\mathcal{V} \equiv \xi\,{}^{\partial\Delta}/_{\partial\xi}$.

A1.2.3 Particular Integral of the vector RTE, solar term

In the treatment of the particular integral solutions of the vector RTE, we use a more traditional substitution method rather than the Green's function formalism of Siewert [*Siewert*, 2000]. This is mainly for reasons of clarity and ease of exposition. Referring to Eq. (A1.1.25), and setting the solar source term direction as $\{-\mu_0, \phi_0\}$, we have from Eq. (A1.2.7) the following source terms in the discrete ordinate directions:

$$\mathbf{Q}_{nm}^{\odot}(x, \pm\mu_i) = \tfrac{\omega_n}{2}\textstyle\sum_{l=m}^{M}\mathbf{P}_l^m(\pm\mu_i)\mathbf{B}_{nl}\,\mathbf{P}_l^m(-\mu_0)\mathbf{F}_{\odot}\mathrm{T}_n\exp[-\lambda_n x]. \qquad \text{(A1.2.22)}$$

Here, we have kept the layer index explicit, and x denotes the vertical optical thickness as measured from the top of layer n; we used the pseudo-spherical treatment of solar beam attenuation (section A1.4.1). The exponential form for the beam attenuation allows us to write the particular solution in the form:

$$\mathbf{I}_{nm}^{\odot}(x, \pm\mu_i) = \mathbf{Z}_n(\pm\mu_i)\mathrm{T}_n\exp[-\lambda_n x], \qquad \text{(A1.2.23)}$$

and by analogy with the homogeneous case, we may define the following vectors of rank $4N_d$:

$$\mathbb{Z}_n^\pm = \left[\mathbf{Z}_n^{\mathrm{T}}(\pm\mu_1), \mathbf{Z}_n^{\mathrm{T}}(\pm\mu_2), \ldots, \mathbf{Z}_n^{\mathrm{T}}\left(\pm\mu_{N_d}\right)\right]^{\mathrm{T}}. \qquad \text{(A1.2.24)}$$

We decouple the equations using sum and difference vectors $\mathbb{R}_n = \mathbb{Z}_n^+ + \mathbb{Z}_n^-$ and $\mathbb{S}_n = \mathbb{Z}_n^+ - \mathbb{Z}_n^-$, and the order is reduced from $8N_d$ to $4N_d$. We obtain the following linear-algebra problem of rank $4N_d$:

$$\mathbb{H}_{\boldsymbol{n}}\mathbb{R}_n = \mathbb{B}_{\boldsymbol{n}}; \quad \mathbb{H}_{\boldsymbol{n}} = \lambda_n^2\mathbb{E} - \mathbb{G}_n; \quad \mathbb{B}_{\boldsymbol{n}} = \left[\mathbb{F}_n^-\mathbb{Q}_n^+ + \tfrac{1}{\lambda_n}\mathbb{Q}_n^-\right]\mathbb{M}^{-1}; \qquad \text{(A1.2.25)}$$

$$\mathbb{Q}_n^\pm = \omega_n\textstyle\sum_{l=m}^{M}\mathbb{P}_{\odot}(l,m)\mathbf{B}_{nl}\mathbf{A}^\pm\mathbb{P}_{\odot}^{\mathrm{T}}(l,m)\,\mathbb{M}^{-1}; \qquad \text{(A1.2.26)}$$

$$\mathbb{P}_{\odot}(l,m) = Diag[\mathbf{P}_l^m(-\mu_0), \mathbf{P}_l^m(-\mu_0), \ldots, \mathbf{P}_l^m(-\mu_0)]^{\mathrm{T}}. \qquad \text{(A1.2.27)}$$

Matrices $\mathbb{F}_n^-$ and $\mathbb{G}_n$ were defined in Eq. (A1.2.10).

This system is solved using the LU-decomposition modules DGETRF and DGETRS from LAPACK; the formal solution is $\mathbb{X}_n^{\odot} = \mathbb{H}_n^{-1}\mathbb{B}_{\boldsymbol{n}}$. The particular integral is completed with the auxiliary equations:

$$\mathbb{Z}_n^{\pm} = \frac{1}{2}\mathbb{M}^{-1}\left[\mathbb{E} \pm \frac{1}{\lambda_n}\mathbb{F}_n^{+}\right]\mathbb{R}_n. \qquad \text{(A1.2.28)}$$

In the scalar LIDORT model, this system has rank N_d. In the vector model, the particular solution consists only of real variables.

Linearizing the particular solution

For this linearization, the most important consideration is the presence of cross-derivatives: in a fully illuminated atmosphere, the particular solution in layer n is differentiable with respect to atmospheric variables ξ_p in all layers $p \leq n$. For the solar beam attenuation (in the pseudo-spherical approximation), transmittance T_n depends on variables ξ_p in layers $p < n$, while average secant λ_n depends on variables ξ_p in layers $p \leq n$. Linearization of the average-secant parameterization is in section A1.4.1. It follows that the solution vectors $\mathbb{Z}_n^{\pm}$ will also depend on ξ_p for $p \leq n$, so *their* linearizations will contain cross-derivatives. Finally, we note that the eigenmatrix $\mathbf{\Gamma}_n$ is constructed from optical properties only defined in layer n, so that $\mathcal{L}_p(\mathbf{\Gamma}_n) = 0, \forall\, p \neq n$.

Differentiation of Eqs. (A1.2.25-A1.2.27) yields a related linear problem:

$$\mathbb{H}_n\mathcal{L}_p(\mathbb{R}_n) = \mathbb{B}'_{np} = \mathcal{L}_p(\mathbb{B}_{\boldsymbol{n}}) - \mathcal{L}_p(\mathbb{H}_{\boldsymbol{n}})\mathbb{R}_n; \qquad \text{(A1.2.29a)}$$

$$\mathcal{L}_p(\mathbb{H}_n) = -\delta_{np}\mathcal{L}_p(\mathbb{G}_n) + 2\lambda_n\mathcal{L}_p(\lambda_n)\mathbb{E}; \qquad \text{(A1.2.29b)}$$

$$\mathcal{L}_p(\mathbb{B}_{\boldsymbol{n}}) = \delta_{np}\left[\mathcal{L}_n(\mathbb{F}_n^{-})\mathbb{Q}_n^{+} + \mathbb{F}_n^{-}\mathcal{L}_n(\mathbb{Q}_n^{+}) + \frac{1}{\lambda_n}\mathcal{L}_n(\mathbb{Q}_n^{-})\right]\mathbb{M}^{-1} - \frac{\mathcal{L}_p(\lambda_n)}{\lambda_n^2}\mathbb{Q}_n^{-}\mathbb{M}^{-1}; \qquad \text{(A1.2.29c)}$$

$$\mathcal{L}_n(\mathbb{Q}_n^{\pm}) = \sum_{l=m}^{M}\left[\mathcal{U}_n\mathbb{P}_{\odot}(l,m)\mathbf{B}_{nl} + \omega_n\mathbb{P}_{\odot}(l,m)\boldsymbol{\mathcal{Z}}_{nl}\right]\mathbf{A}^{\pm}\mathbb{P}_{\odot}^{\mathrm{T}}(l,m)\mathbb{M}^{-1}. \qquad \text{(A1.2.29d)}$$

In Eq. (A1.2.29c), the quantity $\mathcal{L}_n(\mathbb{F}_n^{-})$ comes from Eq. (A1.2.13). This linear system has the same matrix $\mathbb{H}_n$, but with a different source vector $\mathbb{B}'_{np}$. The solution is then found by back-substitution, given that the inverse of $\mathbb{H}_n$ has already been established when solving for $\mathbb{R}_n$. Thus, $\mathcal{L}_p(\mathbb{R}_n) = \mathbb{H}_n^{-1}\mathbb{B}'_n$. Linearization of the particular integral is then completed through differentiation of the auxiliary equations (A1.2.28):

$$\mathcal{L}_p(\mathbb{Z}_n^{\pm}) = \frac{1}{2}\mathbb{M}^{-1}\left[\mathbb{E} \pm \frac{1}{\lambda_n}\mathbb{F}_n^{+}\right]\mathcal{L}_p(\mathbb{R}_n) \pm \frac{1}{2\lambda_n^2}\mathbb{M}^{-1}[\lambda_n\delta_{np}\,\mathcal{L}_n(\mathbb{F}_n^{+}) - \mathcal{L}_p(\lambda_n)\mathbb{F}_n^{+}\,]\mathbb{R}_n. \qquad \text{(A1.2.30)}$$

This completes the RTE solution determination and the corresponding linearizations with respect to atmospheric variables.

A1.2.4 Particular Integral of the vector RTE, thermal emission

In this section, we determine solution of the RTE in the presence of atmospheric thermal emission sources. This formalism is based on the substitution approach used in the original LIDORT work [*Spurr et al*., 2001] and in the DISORT formalism [*Stamnes et al.*, 1988], but with a proper reduction in the order of the corresponding linear algebra system. The Green's function formalism for the scalar LIDORT code may be found in the review paper [*Spurr and Christi*, 2019] for example. We also present a linearization of this solution with respect to the

atmospheric profile variables. Linearization of the thermal solution with respect to the black-body Planck functions is treated in section A1.6.

For isotropic thermal emission in layer n, the source term is $q_n(x) = (1-\omega_n)\eta_n(x)$, where $\eta_n(x)$ is the Planck black-body function expressed as a function of vertical optical thickness within the layer. The phase function for scattering is unity, and the thermal term is only present for the azimuthal series term $m = 0$. There is no polarization, so we require only the (1,1) component of the phase matrix.

In order to obtain solutions, the Planck function is expressed as a polynomial in x across the layer. For convenience, we assume the linear form $\eta_n(x) = a_n + b_n x$. Then, the thermal emission is piecewise continuous through the whole atmosphere and may be completely specified by the Planck functions $\{B_n\}$ at the layer boundaries. Thus, $a_n = B_{n-1}$ and $\Delta_n b_n = B_n - B_{n-1}$, where Δ_n is the whole-layer optical thickness.

We expect the discrete ordinate intensity field to show the same dependency on optical thickness x, so we look for solutions of the form:

$$I_n^{(th)}(x, \pm\mu_i) = T_n^{(1)}(\pm\mu_i) + xT_n^{(2)}(\pm\mu_i). \tag{A1.2.31}$$

We define the following vectors of rank N_d:

$$\mathbb{T}_n^{(s)\pm} = \left[T_n^{(s)}(\pm\mu_1), T_n^{(s)}(\pm\mu_2), \ldots, T_n^{(s)}\left(\pm\mu_{N_d}\right)\right]^{\mathrm{T}}, s = 1, 2. \tag{A1.2.32}$$

We then decouple the resulting RTE with by using sum and difference vectors

$$\mathbb{T}_n^{(1)\pm} = \tfrac{1}{2}\left[\mathbb{H}_n^{(1)} \pm \mathbb{K}_n^{(1)}\right]; \quad \mathbb{T}_n^{(2)\pm} = \tfrac{1}{2}\mathbb{H}_n^{(2)}. \tag{A1.2.33}$$

This reduces the order from $2N_d$ to N_d. Substitution in the RTE and subsequent collection of terms in powers of x yields the following solution using linear algebra of rank N_d:

$$[\mathbb{F}_n^+\mathbb{M}]\mathbb{H}_n^{(1)} = a_n(1-\omega_n)\mathbb{E};\ [\mathbb{F}_n^+\mathbb{M}]\mathbb{H}_n^{(2)} = b_n(1-\omega_n)\mathbb{E};\ [\mathbb{F}_n^-\mathbb{M}]\mathbb{K}_n^{(1)} = -\mathbb{H}_n^{(2)}. \tag{A1.2.34}$$

Here, the $\mathbb{F}_n^{\pm}$ matrices are given by Equation (A1.2.6) but with entries restricted to the (1,1) components of the 4 x 4 polarization matrices. Also in this result, $\mathbb{M} = diag[\mu_1, \mu_2, \ldots \mu_{N_d}]$, and $\mathbb{E}$ is the identity matrix of rank N_d. Linear-algebra determination of the matrix inverses $[\mathbb{F}_n^{\pm}\mathbb{M}]^{-1}$ will yield the solutions.

Linearization of these solutions is straightforward. The Planck functions depend only on the corresponding black-body emission temperatures, and for now we will leave out consideration of weighting functions with respect to temperature profiles, confining our attention to derivatives of the optical properties. In terms of the basic set of linearized optical properties $\mathcal{V}_n \equiv \xi_n\, {}^{\partial\Delta_n}/_{\partial\xi_n}$; $\mathcal{U}_n \equiv \xi_n\, {}^{\partial\omega_n}/_{\partial\xi_n}$; $\mathcal{Z}_{nl} \equiv \xi_n\, {}^{\partial\mathbf{B}_{nl}}/_{\partial\xi_n}$, we have

$$\mathcal{L}_n(a_n) \equiv \xi_n \frac{\partial a_n}{\partial \xi_n} = 0; \quad \mathcal{L}_n(b_n) \equiv \xi_n \frac{\partial b_n}{\partial \xi_n} = -\frac{\mathcal{V}_n b_n}{\Delta_n};$$

Thus, linearizing the three systems in Eq. (A1.2.26), we find

$$[\mathbb{F}_n^+\mathbb{M}].\mathcal{L}_n\left[\mathbb{H}_n^{(1)}\right] = -a_n\mathcal{U}_n\mathbb{E} - \mathcal{L}_n[\mathbb{F}_n^+]\mathbb{M}\mathbb{H}_n^{(1)}; \tag{A1.2.35}$$

$$[\mathbb{F}_n^+\mathbb{M}].\mathcal{L}_n\left[\mathbb{H}_n^{(2)}\right] = -b_n\mathcal{U}_n\mathbb{E} - \mathcal{L}_n(b_n)(1-\omega_n)\mathbb{E} - \mathcal{L}_n[\mathbb{F}_n^+]\mathbb{M}\mathbb{H}_n^{(2)};$$

$$[\mathbb{F}_n^+\mathbb{M}].\mathcal{L}_n\left[\mathbb{K}_n^{(1)}\right] = -\mathcal{L}_n\left[\mathbb{H}_n^{(2)}\right] - \mathcal{L}_n[\mathbb{F}_n^-]\mathbb{K}_n^{(1)}.$$

From the standard solution, we already have the matrix inverses $[\mathbb{F}_n^{\pm}\mathbb{M}]^{-1}$, so these linearizations will proceed rapidly through back substitution using a new set of right-hand column vectors.

Remark. The RTE admits thermal solutions in the absence of scattering. Now, $\omega_n = 0$ and $\mathbb{F}_n^{\pm}\mathbb{M} = \mathbb{E}$, and thermal particular integrals are trivial: $\mathbb{H}_n^{(1)} = a_n\mathbb{E}$, $\mathbb{H}_n^{(2)} = b_n\mathbb{E}$, and $\mathbb{K}_n^{(1)} = -\mathbb{M}^{-1}\mathbb{H}_n^{(2)}$. The linearizations (A1.2.41) still apply, with $\mathcal{L}_n[\mathbb{F}_n^{\pm}] = 0$ throughout. This "thermal transmittance" solution has been included in the VLIDORT model in order that fast "no scattering" solutions to the RTE may be obtained in the thermal infrared and beyond.

A1.3 The post-processed solution

A1.3.1 Boundary value problem (BVP) and linearization

From Section A1.1.3, the complete Stokes vector discrete ordinate solutions in layer *n* may be written:

$$\mathbb{I}_n^{\pm}(x) = \mathbb{D}^{\pm}\sum_{\alpha=1}^{4N_d}\left[\mathfrak{L}_{n\alpha}\mathbb{W}_n^{\pm}e^{-xk_{n\alpha}} + \mathfrak{M}_{n\alpha}\mathbb{W}_n^{\mp}e^{-(\Delta_n - x)k_{n\alpha}}\right] + \mathbb{Z}_n^{\pm}T_{n-1}e^{-x\lambda_n}. \qquad \text{(A1.3.1)}$$

Quantities $\{\mathfrak{L}_{n\alpha}, \mathfrak{M}_{n\alpha}\}$ are *constants of integration* for the homogeneous solutions, and they are determined by the imposition of three boundary conditions as noted in section A1.1.3. For boundary condition (I), we have $\mathbb{I}_n^{\pm}(0) = 1$ for $n = 1$, which yields ($T_0 = 1$):

$$\mathbb{D}^{+}\sum_{\alpha=1}^{4N_d}\left[\mathfrak{L}_{n\alpha}\mathbb{W}_{n\alpha}^{\pm} + \mathfrak{M}_{n\alpha}\mathbb{W}_{n\alpha}^{\mp}\Upsilon_{n\alpha}\right] = -\mathbb{Z}_n^{+}; \qquad (n = 1) \qquad \text{(A1.3.2)}$$

Here, we have used the short-hand $\Upsilon_{n\alpha} \equiv e^{-\Delta_n k_{n\alpha}}$. For boundary condition (II), the continuity at layer boundaries, we have:

$$\mathbb{D}^{\pm}\left\{\sum_{\alpha=1}^{4N_d}\left[\mathfrak{L}_{n\alpha}\mathbb{W}_{n\alpha}^{\pm}\Upsilon_{n\alpha} + \mathfrak{M}_{n\alpha}\mathbb{W}_{n\alpha}^{\mp}\Upsilon_{n\alpha}\right] - \sum_{\alpha=1}^{4N_d}\left[\mathfrak{L}_{p\alpha}\mathbb{W}_{p\alpha}^{\pm} + \mathfrak{M}_{p\alpha}\mathbb{W}_{p\alpha}^{\mp}\Upsilon_{p\alpha}\right]\right\}$$
$$= -\mathbb{Z}_n^{\pm}T_{n-1}\Lambda_n + \mathbb{Z}_p^{\pm}T_{p-1}; \qquad (p = n+1,\ \ n = 2, \ldots N-1) \qquad \text{(A1.3.3)}$$

Here, we have used the short-hand $\Lambda_n \equiv e^{-\Delta_n\lambda_n}$. For the surface condition (III), staying for convenience with the Lambertian condition in Eq. (A1.1.29), we find (for layer $n = N$):

$$\mathbb{D}^{-}\sum_{\alpha=1}^{4N_d}[\mathfrak{L}_{n\alpha}\mathbb{V}_{\alpha}^{-}\Upsilon_{n\alpha} + \mathfrak{M}_{n\alpha}\mathbb{V}_{\alpha}^{+}] = T_{n-1}\Lambda_n[-\mathbb{U}^{-} + 2R_0\mu_0F_{\odot}\mathbb{E}]; \quad n = N. \qquad \text{(A1.3.4)}$$

Here we have defined the following auxiliary quantities:

$$\mathbb{V}_{\alpha}^{\pm} = \mathbb{W}_{n\alpha}^{\pm} - 2R_0\mathbb{M}\mathbb{C}\mathbb{W}_{n\alpha}^{\mp}; \qquad \mathbb{U}^{-} = \mathbb{Z}_n^{-} - 2R_0\mathbb{M}\mathbb{C}\mathbb{Z}_n^{+}; \quad n = N. \qquad \text{(A1.3.5)}$$

Application of Eqs. (A1.3.2-A1.3.4) yields a large, sparse banded linear system with rank $8N_dN$. This system consists only of real variables, and may be written in the symbolic form:

$$\mathfrak{A} \circ \mathfrak{X} = \mathfrak{B}. \qquad \text{(A1.3.6)}$$

Here, $\mathfrak{B}$ is constructed from the right hand side variables in Eqs. (A1.3.2-A1.3.4) and $\mathfrak{A}$ is constructed from suitable combinations of $\{\mathbb{V}_{\alpha}^{\pm}, \mathbb{W}_{n\alpha}^{\pm}, \Upsilon_{n\alpha}\}$. For a visualization of the BVP in the scalar case, see [*Spurr et al.*, 2001]. The vector $\mathfrak{X}$ of integration constants is made up of the unknowns $\{\mathfrak{L}_{n\alpha}, \mathfrak{M}_{n\alpha}\}$ and will be partitioned into real and complex contributions. A schematic of this partitioning is shown in Figure A1.1.

The solution proceeds first by the application of a compression algorithm to reduce the order and eliminate redundant zero entries. LU-decomposition is then applied using the banded-matrix LAPACK routine DGBTRF to find the inverse $\mathfrak{A}^{-1}$, and the final answer $\mathfrak{X} = \mathfrak{A}^{-1} \circ \mathfrak{B}$ is then obtained by back-substitution (using DGBTRS). For the slab problem, boundary condition (II) is absent; the associated linear problem is then solved using the DGETRF/DGETRS combination.

Linearizing Eq. (A1.3.6) with respect to optical or atmospheric variable ξ_p in layer p, we obtain:

$$\mathfrak{A} \circ \mathcal{L}_p(\mathfrak{X}) = \mathfrak{B}'_p = \mathcal{L}_p(\mathfrak{B}) - \mathcal{L}_p(\mathfrak{A}) \circ \mathfrak{X}. \qquad \text{(A1.3.7)}$$

We notice that this is the same linear-algebra problem, but now with a different source vector $\mathfrak{B}'_p$ on the right hand side. Since we already have the inverse $\mathfrak{A}^{-1}$ from the solution to the original BVP, back-substitution gives the linearization $\mathcal{L}_p(\mathfrak{X}) = \mathfrak{A}^{-1} \circ \mathfrak{B}'_p$ of the boundary value constants. Although this linearization is straightforward in concept, there are many algebraic details arising with chain-rule differentiation required to establish $\mathcal{L}_p(\mathfrak{B})$ and $\mathcal{L}_p(\mathfrak{A})$ in Eq. (A1.3.7).

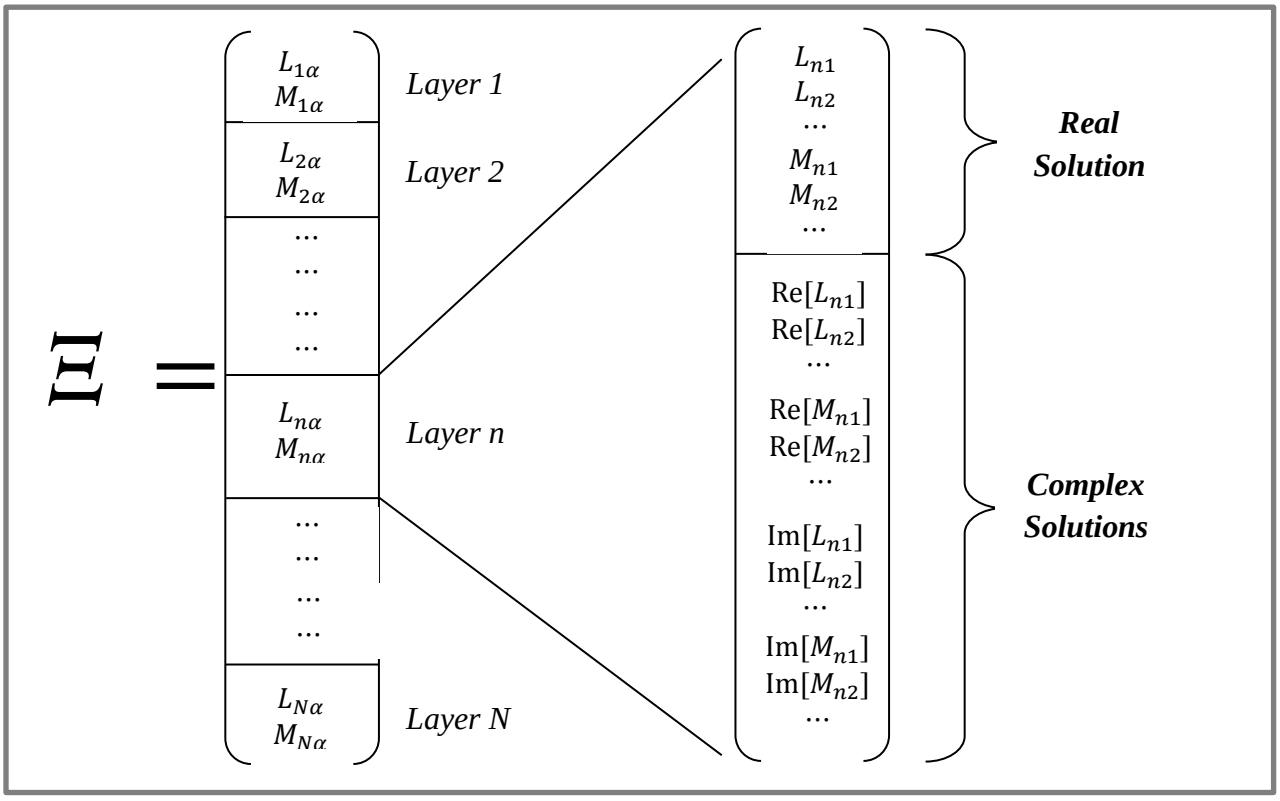

Figure A1.1: Schematic breakdown of the vector of integration constants to be determined as the solution to the boundary value problem in a multilayer atmosphere.

A1.3.2 Source function integration

The source function integration technique is used to determine solutions at off-quadrature polar directions μ and at arbitrary optical thickness values in the multi-layer medium. The technique dates back to the work of Chandrasekhar [*Chandrasekhar*, 1960], and has been demonstrated to be superior to numerical interpolation. We substitute layer discrete ordinate solutions (A1.3.1) into the multiple scattering integral in Eq. (A1.1.22), then integrate over optical thickness. The methodology follows closely that used for the scalar LIDORT code [*Spurr et al.*, 2001; *Spurr*, 2002; *Van Oss and Spurr*, 2002], so long as we remember with the Stokes-vector formulation to use the real part of any quantity derived from combinations of complex-variable entities. Here, we note down the principal results for the upwelling field in the presence of solar scattering.

The Stokes 4-vector solution in layer n at direction μ for optical thickness x (as measured from the top of the layer) is given by:

$$\mathbf{I}_n^-(x,\mu) = \mathbf{I}_n^-(\Delta,\mu)e^{-\frac{\Delta-x}{\mu}} + \mathbf{H}_n^-(x,\mu) + [\mathbf{Z}_n^-(\mu) + \mathbf{Q}_n^-(\mu)]\mathcal{E}_n^-(x,\mu). \qquad \text{(A1.3.8)}$$

The first term is the upward transmission of the lower-boundary Stokes vector field through a partial layer of optical thickness $\Delta - x$. The other three contributions together constitute the *partial layer source term* due to scattered light contributions. The first of these three is due to the homogeneous solutions and has the form:

$$\mathbf{H}_n^-(x,\mu) = \sum_{\alpha=1}^{4N_d}[L_{n\alpha}\mathbf{X}_{n\alpha}^+(\mu)\mathcal{H}_{n\alpha}^{-+}(x,\mu) + M_{n\alpha}\mathbf{X}_{n\alpha}^-(\mu)\mathcal{H}_{n\alpha}^{--}(x,\mu)], \qquad \text{(A1.3.9)}$$

where we have defined the following auxiliary quantities:

$$\mathbf{X}_{n\alpha}^+(\mu) = \frac{\omega}{2}\sum_{l=m}^{LM}\mathbf{P}_l^m(\mu)\mathbf{B}_{nl}\sum_{j=1}^{N_d}w_j\{\mathbf{P}_l^m(\mu_j)\mathbf{X}_{n\alpha}^{\pm}(\mu_i) + \mathbf{P}_l^m(-\mu_j)\mathbf{X}_{n\alpha}^{\pm}(-\mu_i)\}; \qquad \text{(A1.3.10)}$$

$$\mathcal{H}_{n\alpha}^{-+}(x,\mu) = \frac{e^{-xk_{n\alpha}} - e^{-\Delta_n k_{n\alpha}}e^{-\frac{\Delta-x}{\mu}}}{1+\mu k_{n\alpha}};$$

$$\mathcal{H}_{n\alpha}^{--}(x,\mu) = \frac{e^{-(\Delta-x)k_{n\alpha}} - e^{-\frac{\Delta-x}{\mu}}}{1-\mu k_{n\alpha}}. \qquad \text{(A1.3.11a,b)}$$

Here, $\mathbf{X}_{n\alpha}^+(\mu)$ are homogeneous solutions defined at stream cosine μ, and $\mathcal{H}_{n\alpha}^{-+}(x,\mu)$ are the *homogeneous solution multipliers* for the upwelling field. These multipliers arise from the layer optical thickness integration. In (A1.3.9), we consider only the real value of the resulting expressions.

The other two layer source term contributions in (A1.3.8) come from the diffuse and direct solar source scattering respectively. For the solar source terms, all variables are real numbers, and the relevant quantities are:

$$\mathbf{Z}_n^-(\mu) = \frac{\omega}{2}\sum_{l=m}^{LM}\mathbf{P}_l^m(\mu)\mathbf{B}_{nl}\sum_{j=1}^{N_d}w_j\{\mathbf{P}_l^m(\mu_j)\mathbf{Z}_n^-(\mu_j) + \mathbf{P}_l^m(-\mu_j)\mathbf{Z}_n^-(-\mu_j)\}; \qquad \text{(A1.3.12)}$$

$$\mathbf{Q}_n^-(\mu) = \frac{\omega(2-\delta_{m0})}{2}\sum_{l=m}^{LM}\mathbf{P}_l^m(\mu_i)\mathbf{B}_{nl}\,\mathbf{P}_l^m(-\mu_o)\mathbf{I_o}; \qquad \text{(A1.3.13)}$$

$$\mathcal{E}_n^-(x,\mu) = T_{n-1}\frac{e^{-x\lambda_n} - e^{-\Delta_n\lambda_n}e^{-\frac{\Delta_n-x}{\mu}}}{1+\mu\lambda_n}. \qquad \text{(A1.3.14)}$$

These expressions have counterparts in the scalar code (see for example [*Spurr*, 2002]). Similar expressions can be written for post-processing of downwelling solutions. All source term quantities can be expressed in terms of the basic optical property inputs to VLIDORT $\{\Delta_n, \omega_n, \mathbf{B}_{nl}\}$, the pseudo-spherical beam transmittance quantities $\{T_n, \lambda_n\}$, the homogeneous solutions $\{k_{n\alpha}, \mathbf{X}^{\pm}_{n\alpha}\}$, the particular solutions $\mathbf{Z}^{\pm}_n$, and the BVP integration constants $\{L_{n\alpha}, M_{n\alpha}\}$. For thermal source terms, the treatment is similar. For simplicity, we consider integration over the whole layer for the upwelling field. We write:

$$\mathbf{I}^-_n(0,\mu)=\mathbf{I}^-_n(\Delta,\mu)e^{-\frac{\Delta}{\mu}} + \mathbf{H}^-_n(0,\mu) + \mathbf{Z}^-_n(\mu) + \mathbf{D}^-_n(\mu) \qquad \text{(A1.3.15)}$$

Here, $\mathbf{H}^-_n(0,\mu)$ is defined similarly to the expression in (A1.3.9), and the diffuse scattering contribution is given by the following.

$$\mathbf{Z}^-_n(\mu) = \Theta^{(1)}_n(\mu) + \mu\,\Theta^{(2)}_n(\mu)\left(1 - e^{-\frac{\Delta}{\mu}}\right) - \Delta_n\,\Theta^{(2)}_n(\mu)e^{-\frac{\Delta}{\mu}};$$

$$\Theta^{-(s)}_n(\mu) = \frac{\omega}{2}\sum_{l=m}^{LM}\mathbf{P}^m_l(\mu)\beta_{nl}\sum_{j=1}^{N_d} w_j\{\mathbf{P}^m_l(\mu_j)\widetilde{\mathbf{T}}^{-(s)}_n(\mu_j) + \mathbf{P}^m_l(-\mu_j)\widetilde{\mathbf{T}}^{-(s)}_n(-\mu_j)\};$$

(A1.3.16a,b)

In (A1.3.16) we have used components of the thermal discrete ordinate solutions $\widetilde{\mathbf{T}}^{-(s)}_n(\pm\mu_j)$, and reduced the definitions to the (1,1) component of any Mueller matrices (thus, $\mathbf{P}^m_l(\mu)$ become the Legendre polynomials $P_l(\mu)$, and β_{nl} the associated phase function expansion coefficients). The direct term contribution arises from an integration of the Planck source term:

$$\mathbf{D}^-_n(\mu) = (1-\omega_n)\left[a_n + \mu b_n\left(1 - e^{-\Delta/\mu}\right) - \Delta_n b_n(\mu)e^{-\frac{\Delta}{\mu}.}\right] \qquad \text{(A1.3.17)}$$

Linearizations. Derivatives of all these expressions may be determined by differentiation with respect to variable ξ_n in layer n. The end-points of the chain rule differentiation are the linearized optical property inputs $\{\mathcal{V}_n, \mathcal{U}_n, \mathcal{Z}_{nl}\}$ from Eq. (A1.1.33). For linearization of the *homogeneous* post-processing source term in layer n, there is no dependency on any quantities outside of layer n; in other words, $\mathcal{L}_p[\mathbf{H}^-_n(x,\mu)] \equiv 0$ for $p \neq n$. The *particular* solution post-processing source terms in layer n depend on optical thickness values in all layers above and equal to n through the presence of the average secant and the solar beam transmittances, so there will be cross-layer derivatives. However, the chain-rule differentiation method is the same, and requires a careful exercise in algebraic manipulation.

Multiplier expressions (A1.3.11), (A1.3.12) and (A1.3.14) have appeared a number of times in the literature. The linearizations were discussed in [*Spurr*, 2002] and [*Van Oss and Spurr*, 2002], and we need only make two remarks here. Firstly, the real and complex homogeneous solution multipliers are treated separately, with the real part of the complex variable result to be used in the final reckoning. Second, the solar source term multipliers (for example in Eq. (A1.3.14) are *the* same as those in the scalar model.

Linearizations of the thermal post-processed solution are straightforward; details for the scalar solution in LIDORT were noted in the review paper [*Spurr*, 2008].

A1.4 Spherical and single-scatter corrections in LIDORT

A1.4.1 Pseudo-spherical approximation

The pseudo-spherical (P-S) approximation assumes solar beam attenuation for a curved atmosphere. All scattering takes place in a plane-parallel situation. The approximation is a standard feature of many radiative transfer models. We follow the formulation in [*Spurr*, 2002]. Figure A1.2 provides geometrical sketches appropriate to this section.

We consider a stratified atmosphere of optically uniform layers, with extinction optical depths $\Delta_n, n = 1, \ldots N_L$ (the total number of layers). We take points V_{n-1} and V_n on the vertical line (Figure A1.2, upper panel), and the respective solar beam transmittances to these points are then:

$$T_{n-1} = \exp\left[-\sum_{k=1}^{n-1} s_{n-1,k}\Delta_k\right]; \qquad T_n = \exp\left[-\sum_{k=1}^{n} s_{n,k}\Delta_k\right]. \tag{A1.4.1}$$

Here, $s_{n,k}$ is the path distance geometrical factor (Chapman factor), equal to the path distance covered by the V_n beam as it traverses through layer k divided by the corresponding vertical height drop (geometrical thickness of layer k). At the top of the atmosphere, $T_0 = 1$. In the *average secant* parameterization, the transmittance to any intermediate point between V_{n-1} and V_n is parameterized by:

$$T(x) = T_{n-1}\exp[-\lambda_n x], \tag{A1.4.2}$$

where x is the vertical optical thickness measured downwards from V_{n-1} and λ_n the average secant for this layer. Substituting (A1.4.2) into (A1.4.1) and setting $x = \Delta_n$ we find:

$$\lambda_n = \frac{1}{\Delta_n}\left[\sum_{k=1}^{n} s_{n,k}\Delta_k - \sum_{k=1}^{n-1} s_{n-1,k}\Delta_k\right]. \tag{A1.4.3}$$

In the plane-parallel case, we have $\lambda_n = \mu_o^{-1}$ for all n.

<u>*Linearization*</u>: We require derivatives with respect to an atmospheric property ξ_k in layer k. The basic linearized optical property input is the normalized derivative $\mathcal{V}_n$ of the layer optical depth extinction Δ_n. Applying the linearization operator to (A1.4.3) and (A1.4.1), we find:

$$\left.\begin{array}{lll} \mathcal{L}_k[\lambda_n] = \frac{\mathcal{V}}{\Delta_n}(s_{n,n} - \lambda_n); & \mathcal{L}_k[T_n] = 0; & (k = n) \\ \mathcal{L}_k[\lambda_n] = \frac{\mathcal{V}_k}{\Delta_n}(s_{n,k} - s_{n-1,k}); & \mathcal{L}_k[T_n] = -\mathcal{V}_k s_{n-1,k} T_n; & (k < n) \\ \mathcal{L}_k[\lambda_n] = 0; & \mathcal{L}_k[T_n] = 0; & (k > n) \end{array}\right\} \tag{A1.4.4}$$

For the plane-parallel case, we have:

$$\mathcal{L}_k[\lambda_n] = 0\ (\forall k, \forall n); \mathcal{L}_k[T_n] = -\frac{\mathcal{V}_k T_n}{\mu_o}\ (k < n); \qquad \mathcal{L}_k[T_n] = 0\ (k > n); \tag{A1.4.5}$$

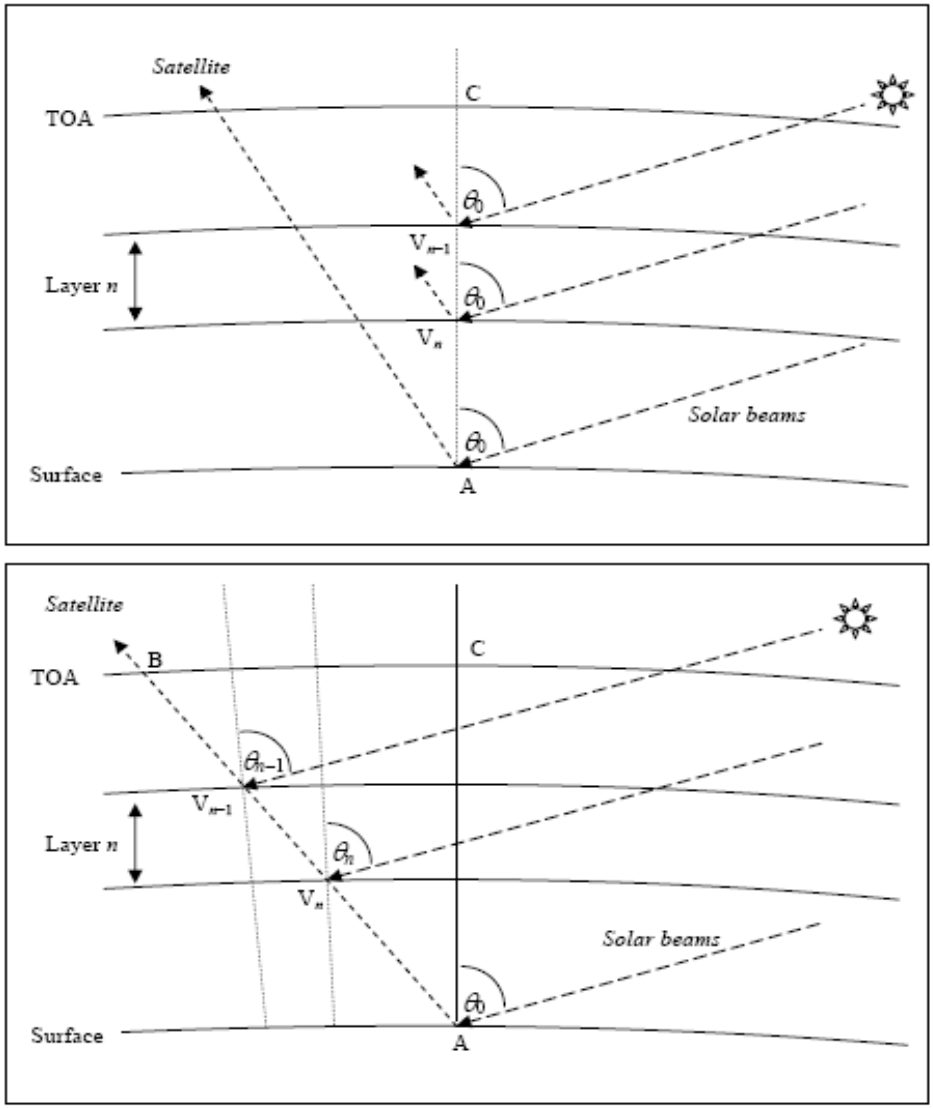

Figure A1.2. (Upper panel) Pseudo-spherical viewing geometry for scattering along the zenith AC. (Lower panel) Line of sight path AB in a curved atmosphere, with viewing and solar angles changing along the path from A to B.

A1.4.2 Exact single scatter solutions

In VLIDORT, we include an exact single-scatter computation based on the Nakajima-Tanaka (NT) procedure [*Nakajima and Tanaka,* 1988]. The internal single scatter computation in VLIDORT will use a truncated subset of the complete scatter-matrix information, the number of usable Legendre coefficient matrices $\mathbf{B}_{nl}$ being limited to $2N_d - 1$ for N_d discrete ordinate streams.

A more accurate computation results when the post-processing calculation of the truncated single scatter contribution (the term $\mathbb{Q}_n^-(\mu)\mathcal{E}_n^-(x,\mu)$ in Eq. (A1.3.11) for example) is suppressed in

favor of an accurate single scatter computation, which uses the complete phase function. This is the so called TMS procedure [*Nakajima and Tanaka*, 1988]. This N-T correction procedure appears in the DISORT Version 2.0 [*Stamnes et al*., 2000] and LIDORT [*Spurr*, 2002] codes. A related computation has been implemented for the doubling-adding method [*Stammes et al.*, 1989].

The (upwelling) post-processed solution in stream direction μ is now written (c.f. Eq. (A1.3.8)):

$$\mathbf{I}_n^-(x,\mu) = \mathbf{I}_n^-(\Delta,\mu)e^{-\frac{\Delta-x}{\mu}} + \mathbf{H}_n^-(x,\mu) + [\mathbf{Z}_n^-(\mu) + \mathbf{Q}_{n,exact}^-(\mu)]\mathcal{E}_n^-(x,\mu), \qquad \text{(A1.4.6)}$$

$$\mathbf{Q}_{n,exact}^-(\mu) = \frac{\omega_n}{4\pi(1-\omega_n f_n)}\mathbf{\Pi}_n(\mu,\mu_o,\phi-\phi_0)\mathbf{F}_\odot. \qquad \text{(A1.4.7)}$$

Note the presence of in the denominator of the expression $(1-\omega_n f_n)$ which is required when the delta-M approximation is in force; f_n is the truncation factor. From section A1.1.1, $\mathbf{\Pi}_n$ is obtained from the scattering matrix $\mathbf{F}_n(\Theta)$ through application of rotation matrices. There is no truncation: $\mathbf{\Pi}_n$ can be constructed to any degree of accuracy using all available *unscaled* Greek matrices $\mathbf{B}_{nl}$.

Linearization. Chain-rule differentiation of Eq. (A1.4.7) yields the linearization of the exact single scatter correction term. Linearization of the multiplier $\mathcal{E}_n^-(x,\mu)$ has already been established. Since the elements of $\mathbf{\Pi}_n$ consist of linear combinations of $\mathbf{B}_{nl}$, the linearization $\mathcal{L}_n(\mathbf{\Pi}_n)$ is straightforward to write down in terms of the inputs $\mathcal{L}_n(\mathbf{B}_{nl})$.

A1.4.3 Sphericity along the line-of-sight

For nadir-geometry satellite instruments with wide-angle off-nadir viewing, one must consider the Earth's curvature along the line of sight from the ground to the satellite. This applies to instruments such as OMI on the Aura platform (swath 2600 km, scan angle 114° at the satellite) [*Levelt et al*., 2006] and GOME-2 (swath 1920 km) [*EPS/METOP*, 1999]. Failure to account for this effect can lead to errors of 5-10% in the satellite radiance for TOA viewing zenith angles in the range 55-70° [*Spurr*, 2003; *Rozanov et al.*, 2000; *Caudill et al*., 1997]. For LIDORT, a simple correction for this effect was introduced for satellite geometries in [*Spurr*, 2003]. The correction involves an exact single scatter calculation along the line of sight from ground to TOA: in this case, Eq. (A1.4.7) is still valid, but now the geometry is changing from layer to layer. The same correction has been adopted for VLIDORT.

In section A1.4.2, scattering was assumed to take place along the nadir, so that the scattering geometry $\Omega \equiv \{\mu_0, \mu, \phi-\phi_0\}$ is unchanged along the vertical. For a slant line-of-sight path (Figure A1.2, lower panel), the scattering geometry varies along the path. For layer n traversed by this path, the upwelling Stokes vector at the layer-top is (to a high degree of accuracy) given by:

$$\mathbf{I}^{\uparrow}(\Omega_{n-1}) \cong \mathbf{I}^{\uparrow}(\Omega_n)T\,(\Omega_n) + \mathbf{\Lambda}_n^{\uparrow}(\Omega_n) + \mathbf{M}_n^{\uparrow}(\Omega_n). \qquad \text{(A1.4.8)}$$

Here, $\mathbf{I}^{\uparrow}(\Omega_n)$ is the upwelling Stokes vector at the layer bottom, $T\,(\Omega_n)$ the layer transmittance along the line of sight, and $\mathbf{\Lambda}_n^{\uparrow}(\Omega_n)$ and $\mathbf{M}_n^{\uparrow}(\Omega_n)$ are the single- and multiple-scatter layer source terms, respectively. The transmittances and layer source terms are evaluated with scattering geometries Ω_n at positions V_n. Eq. (A1.4.8) is applied recursively, starting with the upwelling Stokes vector $\mathbf{I}_{BOA}^{\uparrow}(\Omega_{N_L})$ evaluated at the surface for geometry Ω_{N_L}, and finishing with the field

at top of atmosphere ($n = 0$). The single-scatter layer source terms $\mathbf{\Lambda}_n^{\uparrow}(\Omega_n)$ may be determined through an accurate single scatter calculation (cf. Eq. (A1.4.7)) allowing for changing geometrical angles along the line of sight. To evaluate the multiple scatter sources, we run VLIDORT in "multiple-scatter mode" successively for each of the geometries from Ω_{N_L} to Ω_1, retaining only the appropriate multiple scatter layer source terms, and, for the first VLIDORT calculation with the lowest-layer geometry Ω_{N_L}, the surface upwelling Stokes vector $\mathbf{I}_{BOA}^{\uparrow}(\Omega_{N_L})$.

For N_L layers in the atmosphere, we require N_L separate calls to VLIDORT, and this is much more time consuming that a single call with geometry Ω_{N_L} (this would be the default in the absence of a line-of-sight correction). However, since scattering is strongest near the surface, the first VLIDORT call (with geometry Ω_{N_L}) is the most important as it provides the largest scattering source term $\mathbf{M}_{BOA}^{\uparrow}(\Omega_{N_L})$.

An even simpler line-of-sight correction is to assume that *all* multiple scatter source terms are taken from this first VLIDORT call; in this case, we require only the accurate single scatter calculation to complete $\mathbf{I}_{TOA}^{\uparrow}$. This approximation is known as the "outgoing" sphericity correction; it requires very little extra computational effort compared to a single VLIDORT call. The sphericity correction can also be set up with just two calls to VLIDORT made with the start and finish geometries Ω_{N_L} to Ω_1; in this case, multiple scatter source terms at other geometries are *interpolated* at all levels between results obtained for the two limiting geometries. In the scalar case, accuracies for all these corrections were investigated in [*Spurr*, 2003].

In VLIDORT 2.0, the facility for generating multiple layer source terms has been dropped, as there has been little usage. However, the outgoing sphericity correction is important, and a new formulation has been developed for this release. This has been validated against the TOMRAD code and is applicable also to the vector VLIDORT model. We now describe this.

A1.4.4 FO codes - Single scattering and direct thermal calculations

For Version 2.8, the treatment of single scattering, direct-bounce reflection and direct thermal emission in a curved spherical-shell atmosphere has been revised and simplified. In this section, the exposition applies to the scalar intensity, but the treatment is the same for the VLIDORT implementation.

Dealing first with single scattering in the upwelling direction $\Omega = (\mu, \varphi)$, for a given layer n in an optically-stratified atmospheric model, the vector RTE is (assuming non-refractive geometry):

$$\frac{d\mathbf{I}(x,\Omega)}{dx} = -\mathbf{I}(x,\Omega) + \frac{\omega_n}{4\pi} A_n(x) \mathbf{\Pi}_n^{\uparrow}(\Omega, \Omega_0) \mathbf{F}_{\odot}. \qquad \text{(A1.4.9)}$$

Here, x is the optical thickness coordinate along the line of sight, $\Omega_0 = (-\mu_0, \varphi_0)$ is the solar beam direction, $\mathbf{F}_{\odot} = (F_{\odot}, 0,0,0)^{\mathrm{T}}$ the solar flux vector, $\mathbf{\Pi}_n^{\uparrow}(\Omega, \Omega_0)$ the scattering matrix, $\frac{\omega_n}{4\pi} A_n$ the single scattering albedo, and $A_n(x)$ the solar beam attenuation to the point of scatter. Note that, although the directional dyads $\{\Omega, \Omega_0\}$ will change along the line of sight, the angle of scatter remains constant in straight-line geometry.

In the (V)LIDORT models, layers are optically uniform, so ω_n and $\mathbf{\Pi}_n^{\uparrow}(\Omega, \Omega_0)$ are constant for a given layer n, and $x = \rho_n s$ in terms of the (constant) layer extinction coefficient ρ_n, and path distance s. In terms of the layer vertical height difference h_n and layer vertical optical thickness

Δ_n (one of the basic IOP inputs), $\rho_n = \Delta_n/h_n$. Using path distance as the variable (more convenient, as this is independent of wavelength), we integrate along the line-of-sight from $s = 0$ to $s = D_n$ (at the top boundary of the layer):

$$\mathbf{I}(D_n, \Omega) = \mathbf{I}(0, \Omega)e^{-\rho_n D_n} + \mathbf{S}_n^{\uparrow};\ \ \mathbf{S}_n^{\uparrow} = \frac{\sigma_n}{4\pi}\mathbf{\Pi}_n^{\uparrow}(\Omega, \Omega_0)\mathbf{F}_{\odot} \int_0^{D_n} A_n(s)e^{-\rho_n(D_n - s)}ds. \tag{A1.4.10}$$

This defines the upwelling layer source term $\mathbf{S}_n^{\uparrow}$**.** In addition, we have $\sigma_n = \omega_n\rho_n$ (the scattering coefficient), and the attenuation $A_n(s)$ is found by ray-tracing:

$$A_n(s) = \exp[-\textstyle\sum_{k=1}^{n} d_{nk}(s)\rho_k], \tag{A1.4.11}$$

where $d_{nk}(s)$ are solar path distances through whole layers $k = 1, \ldots n-1$ and the partial distance in layer $k = n$ to the point of scatter.

To obtain the upwelling single-scatter field at all levels in the atmosphere, Eq. (A1.4.10) is applied recursively, starting at the surface; if we write $\mathbf{I}_n^{\uparrow}$ to indicate the upwelling Stokes vector at level boundary n (lower boundary of the layer), then for instance at the top of the atmosphere:

$$\mathbf{I}_0^{\uparrow}(\Omega) = C_{N_d}\mathbf{I}_{Surf}^{\uparrow}(\Omega) + \textstyle\sum_{k=1}^{N_d} C_{k-1}\mathbf{S}_k^{\uparrow}(\Omega);\quad C_n = \prod_{k=1}^{n} e^{-\rho_k D_k};\quad C_0 = 1. \tag{A1.4.12}$$

Similar expressions pertain for output at other levels. The FO-model for upwelling field does include the direct-bounce surface reflectance of the solar beam:

$$\mathbf{I}_{Surf}^{\uparrow}(\Omega) = \frac{1}{\pi}A_{Surf}\mu_0\mathbf{R}(\Omega, \Omega_0)\mathbf{F}_{\odot}, \tag{A1.4.13}$$

with A_{Surf} the solar beam attenuation to the surface, and $\mathbf{R}(\Omega, \Omega_0)$ the BRDF reflection matrix at the surface. In the new FO supplement, there is also the capability to generate fields at intermediate points between level boundaries; the main difference here is that we must now consider partial-layer transmittances and attenuation integrals:

$$\mathbf{I}(s, \Omega) = \mathbf{I}(0, \Omega)e^{-\rho_n s} + \frac{\sigma_n}{4\pi}\mathbf{\Pi}_n^{\uparrow}(\Omega, \Omega_0)\mathbf{F}_{\odot} \int_0^{s} A_n(t)e^{-\rho_n(s-t)}dt. \tag{A1.4.14}$$

Although we have not considered it here, the treatment for downwelling radiation is very similar.

In the FO model, there are three options for computing path attenuations. The first option assumes the atmosphere is plane-parallel. In this case we write $s = (h_n - z)/\mu$ in terms of the vertical height difference z from layer-top and the line-of-sight cosine μ, ,and we have $A_n(s) = T_n \exp[-\rho_n z/\mu_0]$, where T_n is the solar beam transmittance to layer-top. Then we obtain the familiar result:

$$\int_0^{D_n} A_n(s)e^{-\rho_n(D_n - s)}ds = \frac{T_n}{\mu\rho_n}\left[\frac{1-\exp(-\Delta_n\kappa_n)}{\kappa_n}\right];\quad \kappa_n = \frac{1}{\mu_0} + \frac{1}{\mu}. \tag{A1.4.15}$$

The second option allows for curved ray-tracing of the solar beam, but not for the outgoing line-of-sight (the pseudo-spherical approximation). Here we still have $s = (h_n - z)/\mu$, so we could work with vertical coordinates. In the average-secant parameterization used for solar beam attenuation in the multiple-scatter LIDORT and VLIDORT computations, $A_n(s) = T_n \exp[-\lambda_n\rho_n z]$, where the average secant is given by $\lambda_n = \ln[T_n/T_{n+1}]/\rho_n h_n$. In this case, the result in Eq. (A1.4.15) applies, only this time with $\kappa_n = \lambda_n + \frac{1}{\mu}$.

The third choice for the FO model is the fully-spherical situation in which both incoming and outgoing paths are treated for spherical geometry. In this case, the FO model will evaluate attenuation integrals numerically, using a quadrature scheme:

$$\int_0^{D_n} A_n(s)e^{-\rho_n(D_n-s)}ds \cong \sum_{j=1}^{N_q} c_j A_n(s_j)e^{-\rho_n(D_n-s_j)}. \quad \text{(A1.4.16)}$$

Here, the quadrature is $\{s_j, c_j\}, j = 1 \ldots N_q$ taken over the interval $[0, D_n]$. We have found that Gauss-Legendre integration yields accuracy at the 10^{-6} level in most situations, with N_q varying from 5 to 12. However, there are occasions where care must be taken with this procedure. For an optically thick layer below clear skies, solar beam attenuation through such a layer may become vanishingly small. There is then no light reaching the lowest part of the line-of-sight path, and quadrature over interval $[0, D_n]$ will not work. The remedy is to introduce a cutoff distance D_{nc} such that quadrature in (A1.4.15) is over the interval $[D_{nc}, D_n]$. The cutoff is determined as follows: assuming that the layer attenuation $\exp[-d_{nn}(s)\rho_n]$ never falls below a certain threshold value A_{crit}, we use ray-tracing and numerical solution methods to solve for D_{nc} through the equation $A_{crit} = \exp[-d_{nn}(D_{nc})\rho_n]$. We have found $A_{crit} = 10^{-8}$ is a suitable threshold.

The situation with direct thermal emission is simpler. The scalar RTE is

$$\frac{dI(x,\mu)}{dx} = -I(x,\mu) + (1-\omega_n)B_n(x). \quad \text{(A1.4.17)}$$

Here, x is now the vertical optical thickness coordinate measured from the bottom of the layer, and $B_n(x)$ the Planck Function for temperatures in layer n. For the upwelling field, the solution corresponding to Eq. (A1.4.10) is

$$\mathbf{I}(D_n,\mu) = \mathbf{I}(0,\mu)e^{-\rho_n D_n} + (1-\omega_n)\int_0^{D_n} B_n(x)e^{-\rho_n(D_n-s)}ds. \quad \text{(A1.4.18)}$$

There are two choices. The first is the plane-parallel option, with no sphericity along the line-of-sight. Once again, $x = -\rho_n z; s = (h_n - z)/\mu$. Using the linear parameterization $B_n(x) = a_n + b_n s$ in terms of the distance coordinate s, then Eq. (A1.4.18) is then easy to integrate explicitly:

$$\int_0^{D_n} B_n(s)e^{-\rho_n(D_n-s)}ds = \frac{(\rho_n a_n - b_n)(1-e^{-\rho_n D_n})}{\rho_n{}^2} + \frac{b_n D_n}{\rho_n}. \quad \text{(A1.4.19)}$$

In the second choice, the line-of-sight moves through a curved atmosphere, and we must again use the distance quadrature as in Eq. (A1.4.16) to perform the integral in Eq. (A1.4.18).

Building the field recursively using Eq. (A1.4.12) also applies in the thermal case, except that the surface term is now given by $I^{\uparrow}_{Surf}(\Omega) = B_{Surf}E(\mu)$, with emissivity $E(\mu)$ and surface Planck function B_{Surf}. Downwelling treatment for direct thermal radiation unfolds in an analogous way.

Linearizations. We note that the FO fields are differentiable with respect to any basic set of optical properties that characterize the RT problem. In layer n, we assume that the IOPs $\{\Delta_n, \omega_n, \mathbf{\Pi}_n(\Omega,\Omega_0)\}$ have known analytic derivatives $\{\dot{\Delta}_n, \dot{\omega}_n, \dot{\mathbf{\Pi}}_n(\Omega,\Omega_0)\}$ with respect to variable ξ_n in layer n. Differentiation of Eq. (A1.4.14) yields:

$$\dot{\mathbf{I}}(D_n,\Omega) = \left[\dot{\mathbf{I}}(0,\Omega) - \dot{\rho}_n D_n \mathbf{I}(0,\Omega)\right]e^{-\rho_n D_n} + \dot{\mathbf{S}}^{\uparrow}_n; \quad \text{(A1.4.20a)}$$

$$\dot{\mathbf{S}}_n^{\uparrow} = \frac{1}{4\pi}\left[\dot{\sigma}_n \mathbf{\Pi}_n^{\uparrow}(\Omega,\Omega_0) + \sigma_n \dot{\mathbf{\Pi}}_n^{\uparrow}(\Omega,\Omega_0)\right]\mathbf{F}_{\odot} \int_0^{D_n} A_n(s) e^{-\rho_n(D_n-s)} ds$$
$$+ \frac{\sigma_n}{4\pi}\mathbf{\Pi}_n^{\uparrow}(\Omega,\Omega_0)\mathbf{F}_{\odot} \int_0^{D_n}\left[\dot{A}_n(s) - \dot{\rho}_n(D_n-s)A_n(s)\right] e^{-\rho_n(D_n-s)} ds. \qquad \text{(A1.4.20b)}$$

In terms of linearized IOPs, we have $\dot{\rho}_n = \dot{\Delta}_n/h_n$, and $\dot{\sigma}_n = \dot{\rho}_n\omega_n + \rho_n\dot{\omega}_n$. Equation (A1.4.20b) contains some new integrals for the attenuations; the derivative attenuation from Eq. (A1.4.11) is:

$$\dot{A}_n(s) = -d_{nn}(s)\dot{\rho}_n A_n(s). \qquad \text{(A1.4.21)}$$

Additionally, there are cross-layer derivatives of Eq. (A1.4.14), since the attenuation depends on optical properties in layers $k < n$. If quantity ξ_k in layer k gives rise to optical property derivatives $\partial\rho_k/\partial\xi_k$, then (using a "prime" symbol for $\partial/\partial\xi_k$)

$$\mathbf{I}'(D_n,\Omega) = \mathbf{I}'(0,\Omega)e^{-\rho_n D_n} + \frac{\sigma_n}{4\pi}\mathbf{\Pi}_n^{\uparrow}(\Omega,\Omega_0)\mathbf{F}_{\odot} \int_0^{D_n} A'_{nk}(s) e^{-\rho_n(D_n-s)} ds. \qquad \text{(A1.4.22)}$$

Here, $A'_{nk}(s) = -d_{nk}(s)\rho'_k A_n(s)$, for $k < n$. Integrals with derivatives of the attenuations will have analytical expressions for the plane-parallel option and the pseudo-spherical option with the average-secant parameterization. These integrals have already cropped up in the full RTE linearizations. For the other option with full sphericity, integrals in Eq. (A1.4.22) are done using the distance quadrature as noted above.

Solution linearization of the complete single-scatter field then follows from the chain-rule differentiation of the recurrence relation Eq. (A1.4.12) and others similar to it. We note in particular the surface attenuation in Eq. (A1.4.13) will have derivatives from every layer.

One final consideration is the surface-property linearization of the direct-reflection in Eq. (A1.4.13). If the BRDF has derivative $\partial/\partial W$ (indicated below with a "double prime" symbol), with respect to some surface quantity W (e.g. wind speed for ocean glitter), then there will be Jacobians such as the following:

$$\mathbf{I}_0^{\uparrow\,\prime\prime}(\Omega) = C_{N_d}\mathbf{I}_{Surf}^{\uparrow\,\prime\prime}(\Omega); \quad \mathbf{I}_{Surf}^{\uparrow\,\prime\prime}(\Omega) = \frac{1}{\pi}A_{Surf}\mu_0\mathbf{R}''(\Omega,\Omega_0)\mathbf{F}_{\odot}. \qquad \text{(A1.4.23)}$$

Linearization of the direct thermal FO field has two aspects. The first is differentiation with respect to the usual set of optical property variables – in a manner not unrelated to the above treatment for the SS field, we may differentiate the results in Eqs. (A1.4.17)-(A1.4.19), noting the need for additional quadrature integration involving the Plank functions. The other consideration is differentiation with respect to the Planck functions themselves – an important factor when considering temperature Jacobians in the thermal regime. This issue was dealt with in section A1.2.4 and the facility developed there is appropriate to the present case.

A1.5 Bulk (total column) atmospheric Jacobians.

One of the most important applications for VLIDORT has been in forward model simulations for ozone profile and total column retrieval. The use of total column as a proxy for the ozone profile was recognized a number of years ago by scientists at NASA, and column-classified ozone profile climatologies were created for the TOMS Version 7 [*Wellemayer et al.*, 1997] and Version 8 retrieval algorithms [*Bhartia*, 2003]. If the profile is represented as a set $\{U_j\}$ of partial columns in Dobson Units [DU], then the total column (also in [DU]) is $C = \sum_j U_j$. For two

adjacent TOMS profiles $\{U_j^{(1)}\}$ and $\{U_j^{(2)}\}$ with total columns $C^{(1)}$ and $C^{(2)}$, we define an intermediate profile with column amount C according to:

$$U_j(C) = \left(\frac{C-C^{(1)}}{C^{(2)}-C^{(1)}}\right) U_j^{(2)} + \left(\frac{C^{(2)}-C}{C^{(2)}-C^{(1)}}\right) U_j^{(1)}. \qquad \text{(A1.5.1)}$$

This defines the profile-column map; it is linear in C. Total column weighting functions are related to profile Jacobians by means of chain rule differentiation and the partial derivative:

$$\frac{\partial U_j(C)}{\partial C} = \left(\frac{U_j^{(2)}-U_j^{(1)}}{C^{(2)}-C^{(1)}}\right). \qquad \text{(A1.5.2)}$$

This map allows us to interpolate smoothly between profile entries in the climatology. In effect, we are drawing on an ensemble of possible profiles of which the climatology is a sample. Other maps are possible. TOMS Version 8 profiles are specified for 18 latitude bands from pole to pole (10° intervals), and for each month of the year.

Suppose now we have a Rayleigh atmosphere with Rayleigh scattering cross-section $\sigma^{Ray}(\lambda)$, air column density D_p in layer p, ozone partial columns U_p, and temperature-dependent ozone cross sections $\sigma_p^{O3}(\lambda)$; then the bulk property IOPs are:

$$\Delta_p = \sigma^{Ray}(\lambda)D_p + \sigma_p^{O3}(\lambda)U_p; \qquad \omega_p = \frac{\sigma^{Ray}(\lambda)D_p}{\Delta_p}; \qquad \text{(A1.5.3)}$$

Differentiating (A1.5.2) with respect to U_p gives the linearized IOP inputs for the profile Jacobian:

$$\frac{\partial \Delta_p}{\partial U_p} = \sigma_p^{O3}(\lambda); \qquad \frac{\partial \omega_p}{\partial U_p} = -\frac{\omega_p}{\Delta_p}\frac{\partial \Delta_p}{\partial U_p}. \qquad \text{(A1.5.4)}$$

Finally, we compute the column Jacobian using the chain rule:

$$K_{col}(\Omega) \equiv \frac{\partial I(0,\Omega)}{\partial C} = \sum_{p=1}^{n} \frac{\partial I(0,\Omega)}{\partial U_p}\frac{\partial U_p}{\partial C}. \qquad \text{(A1.5.5)}$$

Note the use of the profile-column mapping derivatives $\frac{\partial U_p}{\partial C}$. Merely adding up the partial column weighting functions is equivalent to assuming that the response of the TOA field to variations in total ozone is the same for all layers – the profile shape remains the same. Equation (A1.5.5) is the correct formula to account for shape variation.

It is perfectly possible to set up VLIDORT to deliver a set of *profile* Jacobians; a *column* weighting function would then be created *externally* from the sum in Eq. (A1.5.5). This is not very efficient, since for a 13-layer atmosphere we must calculate 13 separate profile weighting functions and then sum them. However, a facility was introduced in the scalar LIDORT code Version 2.5 to have LIDORT calculate the column Jacobian directly; in effect, the summation in Eq. (A1.5.5) is done *internally*. This is a much more efficient procedure. In this case the linearized IOP inputs are expressed in terms of the profile-column mapping derivatives:

$$\frac{\partial \Delta_p}{\partial C} = \sigma_p^{O3}(\lambda)\frac{\partial U_p}{\partial C}; \qquad \frac{\partial \omega_p}{\partial C} = -\frac{\omega_p}{\Delta_p}\sigma_p^{O3}(\lambda)\frac{\partial U_p}{\partial C}. \qquad \text{(A1.5.6)}$$

This feature has been retained in all LIDORT Version 3 codes, and the single-scatter corrections (outgoing and nadir), surface treatments and performance enhancements (in particular the linearization of the reduced BVP problem) have been upgraded to ensure that the column differentiation is done internally inside LIDORT if the requisite flag is turned on for column linearization. The model will generate either profile or column Jacobians for atmospheric quantities.

A1.6 Facility for blackbody Jacobians

A1.6.1. Introduction

In this section, we are concerned with thermal solutions to the RTE for isotropic equilibrium thermal emission in the atmosphere and from the surface. The source of emission is the Planck black-body function $B_n(x)$ which is dependent on the optical thickness x in layer n of our stratified atmosphere.

If (as is usual) the Planck function is parameterized linearly, then $B_n(x) = a_n + b_n x$, with $a_n = B_{n-1}$ and $b_n = \frac{B_n - B_{n-1}}{\Delta_n}$ in terms of the Planck functions B_{n-1} and B_n at the top and bottom boundaries of the layer. The set $\{B_n\}$ for $n = 0, 1, \cdots N_L$ (along with the surface Planck function B_{sur}) are then the fundamental thermal-emission inputs to the RT model.

Following the introduction, this section has three parts. First, we review the solution for the RTE in the presence of thermal atmospheric sources focusing on the power-series methodology used in VLIDORT (which is different from the Green's function approach used in LIDORT). We also summarize the linearization of thermal solutions with respect to the usual atmospheric quantities.

The second part is concerned with one of the last remaining analytic Jacobian derivations for VLIDORT, namely, the derivation of radiation-field Jacobians with respect to Planck Functions specified at layer boundaries. Version 2.8 of VLIDORT was given this capability. For given wave number, these Planck functions depend solely on the corresponding temperatures at level boundaries, so that this BB-Jacobian derivation is ultimately of great importance in deriving analytic temperature Jacobians in the thermal scattering regime. In this part, we carry out an explicit linearization of the complete thermal solution with respect to the Planck functions.

In the third part, we show how a complete set of level-boundary temperature derivatives can be determined for the thermal scattering regime from VLIDORT outputs and suitable chain-rule dependencies. This part is based on material in [*Spurr and Christi*, 2014], in which the procedure for generation of VLIDORT-based Jacobians with respect to temperatures specified at *level* boundaries was discussed. [VLIDORT is a linearized RT model for atmospheres with optically-uniform layer stratification, delivering *layer* Jacobians with respect to layer optical properties.] Level-boundary temperature Jacobians are then found using the functional dependence of these layer properties on level-boundary temperatures and the chain-rule applied to VLIDORT Jacobian output. In the solar regime, temperature dependence is restricted to optical properties, but the additional Planck-function temperature dependence in the presence of thermal sources needs special consideration, as described in this part.

A1.6.2 Thermal regime solutions in VLIDORT

Isotropic thermal emission is unpolarized, so without loss of generality we solve the RTE only for the intensity field. We will derive the thermal emission discrete-ordinate particular integral and the associated contributions to the post-processed radiation. In LIDORT, this process is done use the Green's function formalism – here for VLIDORT we deploy a more traditional solution.

Then the azimuth-independent (Fourier $m = 0$) RTE in layer n in the presence of thermal sources may be written:

$$\mu \frac{dI(x,\mu)}{dx} = -I(x,\mu) + \frac{\omega_n}{2}\int_{-1}^{1} \Phi_n(\mu,\mu')I(x,\mu')d\mu' + (1-\omega_n)B_n(x), \qquad \text{(A1.6.1)}$$

where $\Phi_n(\mu,\mu')$ is the (azimuth-independent) contribution to the Fourier-series expansion of the scattering phase function, ω_n is the layer single scattering albedo, x the optical thickness measured from the top of the atmospheric layer, and $B_n(x)$ the Planck function source in that layer. Scattering properties $\{\omega_n, \Phi_n\}$ are assumed independent of x; our stratified atmosphere has N_L layers in total. We drop the Fourier index m.

Accordingly, we look for particular integrals of the form:

$$I_n(x, \pm\mu_j) = \mathcal{T}_n^{(1)}(\pm\mu_j) + x\mathcal{T}_n^{(2)}(\pm\mu_j) \qquad \text{(A1.6.2)}$$

Here $\{\pm\mu_j\}, j = 1, \ldots N_d$ are quadrature streams in the downwelling (+) and upwelling (-) polar hemispheres, with $\{c_j\}, j = 1, \ldots N_d$ the corresponding quadrature weights. Eq. (A1.6.2) is substituted in Eq. (A1.6.1) and the multiple-scattering integral approximated in the usual manner by the discrete-ordinate quadrature. We then equate powers of x**,** and the resulting coupled sets of linear differential equations are then solved by linear-algebra determinations of $\mathcal{T}_n^{(1)}$ and $\mathcal{T}_n^{(2)}$.

We use sum-and difference vectors to reduce the system rank from $2N_d$ to N_d:

$$\mathcal{T}_n^{(1)}(\pm\mu_j) = \tfrac{1}{2}\left[\mathcal{H}_n^{(1)}(\mu_j) \pm \mathcal{J}_n^{(1)}(\mu_j)\right]; \quad \mathcal{T}_n^{(2)}(\mu_j) = \mathcal{T}_n^{(2)}(-\mu_j) = \tfrac{1}{2}\left[\mathcal{H}_n^{(2)}(\mu_j)\right]. \qquad \text{(A1.6.3)}$$

After substitution, the following three linear-algebra problems are to be solved in succession:

$$\mathbb{S}_n\mathbb{H}_n^{(1)} = a_n'\mathbb{E}; \qquad \mathbb{S}_n\mathbb{H}_n^{(2)} = b_n'\mathbb{E}; \qquad \mathbb{D}_n\mathbb{J}_n^{(1)} = \mathbb{H}_n^{(2)}. \qquad \text{(A1.6.4)}$$

Here, $\mathbb{H}_n^{(1)}$ is the vector with components $\mathcal{H}_n^{(1)}(\mu_j)$, with similar definitions for $\mathbb{J}_n^{(1)}$ and $\mathbb{H}_n^{(2)}$, $\mathbb{E}$ is a vector with all entries equal to 1, and $a_n' = 2(1-\omega_n)a_n$ with $b_n' = 2(1-\omega_n)b_n$. We will use the notation

The matrices $\mathbb{S}_n$ and $\mathbb{D}_n$ are closely related to similar quantities used to find the homogeneous solutions Eqs. (A1.2.4) and are given by:

$$\{\mathbb{S}_n\}_{ij} = \delta_{ij} - \frac{\omega_n}{2}\sum_{l=0}^{2N_d-1}\beta_{nl}\left[P_l(\mu_i)P_l(\mu_j) + P_l(\mu_i)P_l(-\mu_j)\right]c_j. \qquad \text{(A1.6.5a)}$$

$$\{\mathbb{D}_n\}_{ij} = -\frac{1}{\mu_i}\delta_{ij} + \frac{\omega_n}{2}\sum_{l=0}^{2N_d-1}\beta_{nl}\frac{1}{\mu_i}\left[P_l(\mu_i)P_l(\mu_j) + P_l(\mu_i)P_l(-\mu_j)\right]c_j. \qquad \text{(A1.6.5b)}$$

This completes the discrete ordinate solution. For the post processing step(source function integration), we define solution vectors at arbitrary polar direction μ, just as we did with the solar term particular integral:

$$\mathcal{H}_n^{(1)}(\pm\mu) = \frac{\omega_n}{2}\sum_{l=0}^{2N_d-1}\beta_{nl}P_l(\mu)\sum_{j=1}^{N_d}P_l(\pm\mu_j)c_j\mathcal{H}_n^{(1)}(\mu_j). \qquad \text{(A1.6.6)}$$

Similar definitions for $\mathcal{H}_n^{(2)}(\pm\mu)$ and $\mathcal{J}_n^{(1)}(\pm\mu)$, and we can use them to create the complete thermal post-processed solutions $\mathcal{T}_n^{(1)}(\pm\mu) + x\mathcal{T}_n^{(2)}(\pm\mu)$, for the upwelling (+) and downwelling (-)fields. Upon integrating over optical depth from one level boundary to the other, we find for example that the whole-layer upwelling and downwelling source field contributions from thermal emission are:

$$S_n^{\uparrow}(\mu) = \left(\mathcal{T}_n^{(1)}(\mu) + \mu\mathcal{T}_n^{(2)}(\mu)\right)\left(1-\exp[-\tfrac{\Delta_n}{\mu}]\right) - \Delta_n\,\mathcal{T}_n^{(2)}(\mu)\exp\left[-\tfrac{\Delta_n}{\mu}\right]; \qquad \text{(A1.6.7a)}$$

$$S_n^{\downarrow}(\mu) = \left(\mathcal{T}_n^{(1)}(-\mu) - \mu\mathcal{T}_n^{(2)}(-\mu)\right)\left(1-\exp[-\tfrac{\Delta_n}{\mu}]\right) - \Delta_n\mathcal{T}_n^{(2)}(-\mu); \qquad \text{(A1.6.7b)}$$

Similar expressions can be derived for the thermal radiation field at partial-layer output levels.

For the optical property linearization, we consider linearization with respect to an atmospheric variable ξ_n in layer n, based on knowledge of the IOP derivatives:

$$\mathcal{V}_n \equiv \mathcal{L}[\Delta_n] = \xi_n\frac{\partial\Delta_n}{\partial\xi_n}; \quad \mathcal{U}_n \equiv \mathcal{L}[\omega_n] = \xi_n\frac{\partial\omega_n}{\partial\xi_n}; \quad \mathcal{Z}_{nl} \equiv \mathcal{L}[\beta_{nl}] = \xi_n\frac{\beta_{nl}}{\partial\xi_n}. \qquad \text{(A1.6.8)}$$

Referring to the 3 linear-algebra problems in Eq. (A1.6.4), we can differentiate them formally:

$$\mathcal{L}\left[\mathbb{H}_n^{(1)}\right] = -\mathbb{S}_n^{-1}\left(\mathcal{L}[\mathbb{S}_n]\mathbb{H}_n^{(1)} - 2\mathcal{U}_n a_n\right); \qquad \text{(A1.6.9a)}$$

$$\mathcal{L}\left[\mathbb{H}_n^{(2)}\right] = -\mathbb{S}_n^{-1}\left(\mathcal{L}[\mathbb{S}_n]\mathbb{H}_n^{(2)} - 2\mathcal{U}_n b_n\right); \qquad \text{(A1.6.9b)}$$

$$\mathcal{L}\left[\mathbb{J}_n^{(1)}\right] = \mathbb{D}_n^{-1}\left(\mathcal{L}\left[\mathbb{H}_n^{(2)}\right] - \mathcal{L}[\mathbb{D}_n]\mathbb{J}_n^{(1)}\right). \qquad \text{(A1.6.9c)}$$

Quantities $\mathcal{L}[\mathbb{D}_n]$ and $\mathcal{L}[\mathbb{D}_n]$ are found easily from explicit differentiation of Eqs. (A.1.6.5), and the inverse matrices $\mathbb{S}_n^{-1}$ and $\mathbb{D}_n^{-1}$ are already known from solution of the original thermal particular integral. This procedure is of course similar to that for the solar field, but with one important difference, namely, there are no cross-derivatives (dependencies in layer n on quantities varying in layers $p \neq n$). Note also that the thermal coefficients $\{a_n, b_n\}$are not dependent on optical properties, so their derivatives with respect to ξ_n are zero.

These linearized particular integrals can then be used to construct the right-hand vector appropriate to the linearized boundary value problem (BVP) – the methodology is similar to that used for the solar field linearization, and we do not go into details here.

A1.6.3. Planck function Jacobians

Here we consider derivation of Jacobians with respect to the Black Body Planck functions $\{B_n\}, n = 0,1,2 \ldots N_L$. Given coefficients $a_n = B_{n-1}$ and $b_n = (B_n - B_{n-1})/\Delta_n$ appropriate to the linear parameterization $B_n(x) = a_n + b_n x$, the trick here is to express thermal solutions in each layer n in terms of the level boundary quantities B_{n-1} and B_n. This turns out to be a straightforward exercise, helped by the fact that matrices $\mathbb{S}_n$ and $\mathbb{D}_n$ in Eqs. (A1.6.5) have no

dependence on the Planck functions, from which it follows from Eqs. (A1.6.4) that every element of the vector $\mathbb{H}_n^{(1)}$ will have the same dependence on B_{n-1}, while every element of vectors $\mathbb{H}_n^{(2)}$ and $\mathbb{J}_n^{(1)}$ will have the same dependence on B_{n-1} and B_n. Without going into too much detail, we may then write

$$\mathbb{T}_n^{\pm}(x) = B_{n-1}\,\mathbb{P}_n^{\pm}(x) + B_n\,\mathbb{Q}_n^{\pm}(x). \tag{A1.6.10}$$

For the discrete ordinate vectors at optical thickness x, where vectors $\mathbb{P}_n^{\pm}(x)$ and $\mathbb{Q}_n^{\pm}(x)$ have been constructed from the above re-arrangement. We remark also that the form of the post processed solution vectors in Eq. (A1.6.6) will also allow them to be expressed similarly as a linear combination of B_{n-1} and B_n.

In order to proceed with this linearization, we first make a recapitulation of the BVP. The discrete ordinate solution of the RTE in layer *n* is a linear combination of the homogeneous solutions plus the thermal particular integral given above:

$$\mathbb{I}_n^{\pm}(x) = \sum_{\alpha=1}^{N_d}\left[L_{n\alpha}\mathbb{X}_{n\alpha}^{\pm}e^{-xk_{n\alpha}} + M_{n\alpha}\mathbb{X}_{n\alpha}^{\mp}e^{-(\Delta_n - x)k_{n\alpha}}\right] + \mathbb{T}_n^{\pm}(x). \tag{A1.6.11}$$

Here, the constants of integration $\{L_{n\alpha}, M_{n\alpha}\}$ will be determined by imposition of the usual three boundary conditions: (1) at the top boundary $n = 0$ there is no diffuse downwelling radiation; (2) at the bottom boundary $n = N$ there is a surface reflection condition plus surface emission; and (3) there is continuity of the diffuse field at intermediate layer boundaries $n = 1, \ldots N-1$.

The BVP problem $\mathbb{M}\cdot\mathbb{V} = \mathbb{Y}$ for the vector $\mathbb{V}$ of all unknown layer integration constants; here, matrix $\mathbb{M}$ is a sparsely populated band-matrix constructed solely from RTE homogeneous solutions, while vector $\mathbb{Y}$ expresses the boundary conditions applied to particular integrals. For the thermal case under discussion here, we will be more explicit, assuming for conciseness that the lower boundary is dark (no reflection); surface emissivity is then unity (in the following, B_{sur} is the surface emission Planck function). The *explicit* form for $\mathbb{Y}$ may be written:

$$\mathbb{Y} = \begin{pmatrix} -\mathbb{T}_1^{+}(0) \\ \mathbb{T}_2^{\pm}(0) - \mathbb{T}_1^{\pm}(\Delta_1) \\ \ldots \\ \mathbb{T}_N^{\pm}(0) - \mathbb{T}_{N-1}^{\pm}(\Delta_{N-1}) \\ \mathbb{T}_N^{-}(\Delta_N) + \mathbb{E}B_{sur} \end{pmatrix} = \begin{pmatrix} -B_0\,\mathbb{P}_1^{+} - B_1\,\mathbb{Q}_1^{+} \\ -B_2\,\mathbb{Q}_2^{\pm} - B_0\,\mathbb{R}_1^{\pm} + B_1\left(\mathbb{P}_2^{\pm} - \mathbb{W}_1^{\pm}\right) \\ \ldots \\ -B_N\,\mathbb{Q}_N^{\pm} - B_{N-2}\,\mathbb{R}_{N-1}^{\pm} + B_{N-1}\left(\mathbb{P}_N^{\pm} - \mathbb{W}_{N-1}^{\pm}\right) \\ B_{N-1}\,\mathbb{R}_N^{-} + B_N\mathbb{W}_N^{-} + \mathbb{E}B_{sur} \end{pmatrix}. \tag{A1.6.12}$$

Here, $\mathbb{E}$ is vector of rank N_d with unit entries; this represents the emissivity. We have also used the short-hand $\mathbb{P}_n^{\pm} = \mathbb{P}_n^{\pm}(0)$, $\mathbb{Q}_n^{\pm} = \mathbb{Q}_n^{\pm}(0)$, $\mathbb{R}_n^{\pm} = \mathbb{P}_n^{\pm}(\Delta_n)$, and $\mathbb{W}_n^{\pm} = \mathbb{Q}_n^{\pm}(\Delta_n)$.

The solution vector $\mathbb{V} = \mathbb{M}^{-1}\cdot\mathbb{Y}$ gives us $\{L_{n\alpha}, M_{n\alpha}\}$ for all layers; we note that each of these quantities is dependent on the complete set $\{B_n\}, n = 0, \ldots N$, and also on B_{sur}.

Now, from Eq. (A1.6.10), the derivatives of the particular integrals at level boundaries could not be simpler:

$$\frac{\partial\mathbb{T}_2^{\pm}(0)}{\partial B_{n-1}} = \mathbb{P}_n^{\pm};\ \frac{\partial\mathbb{T}_2^{\pm}(0)}{\partial B_n} = \mathbb{Q}_n^{\pm}; \tag{A1.6.13a}$$

$$\frac{\partial\mathbb{T}_2^{\pm}(\Delta_n)}{\partial B_{n-1}} = \mathbb{R}_n^{\pm};\ \frac{\partial\mathbb{T}_2^{\pm}(\Delta_n)}{\partial B_n} = \mathbb{W}_n^{\pm}. \tag{A1.6.13b}$$

Given boundary-value problem $\mathbb{M} \cdot \mathbb{V} = \mathbb{Y}$ and its solution $\mathbb{V} = \mathbb{M}^{-1} \cdot \mathbb{Y}$, the linearization of this is $\delta_k \mathbb{V} = \mathbb{M}^{-1} \cdot \delta_k \mathbb{Y}$, where we have used the shorthand $\delta_k = \partial / \partial B_k$. Matrix $\mathbb{M}$ has no dependence on the Planck functions ($\delta_k \mathbb{M} = \mathbf{0}$), and $\delta_k \mathbb{Y}$ may be written down by an explicit examination of the entries in Eq. (A1.6.10) and the particular integral derivatives in Eqs. (A1.6.13). Indeed, for the first two levels:

$$\delta_0 \mathbb{Y} = \begin{pmatrix} -\mathbb{P}_1^+ \\ -\mathbb{R}_1^+ \\ 0 \\ 0 \\ \ldots \\ 0 \end{pmatrix}; \quad \delta_1 \mathbb{Y} = \begin{pmatrix} -\mathbb{Q}_1^+ \\ \mathbb{P}_2^\pm - \mathbb{W}_1^\pm \\ -\mathbb{R}_2^+ \\ 0 \\ \ldots \\ 0 \end{pmatrix}., \text{etc ...} \tag{A1.6.14}$$

The trick here is to make sure that the vector entries $\delta_k \mathbb{Y}$ are filled up correctly - a variable defined at level boundary *k* will have an effect on the two adjacent layers above and below this boundary. Since we have the inverse matrix $\mathbb{M}^{-1}$ from the original solution of the radiance field, the linearized vector $\delta_k \mathbb{V}$ is readily computed.

The linearized discrete ordinate solution in layer n with respect to the Planck function B_k at level k can now be written:

$$\frac{\partial \mathbb{I}_n^\pm(x)}{\partial B_k} = \sum_{\alpha=1}^N \left[\frac{\partial L_{n\alpha}}{\partial B_k} \mathbb{X}_{n\alpha}^\pm e^{-xk_{n\alpha}} + \frac{\partial M_{n\alpha}}{\partial B_k} e^{-(\Delta_n - x)k_{n\alpha}} \mathbb{X}_{n\alpha}^\mp \right] + \frac{\partial \mathbb{T}_n^\pm(x)}{\partial B_k}. \tag{A1.6.15}$$

Here the derivatives $\left\{ \frac{\partial L_{n\alpha}}{\partial B_k}, \frac{\partial M_{n\alpha}}{\partial B_k} \right\}$ emerge from the $\delta_k \mathbb{V}$ vector, while $\frac{\partial \mathbb{T}_n^\pm(x)}{\partial B_k}$ follows from the explicit differentiation. As noted above, derivatives $\frac{\partial \mathbb{T}_n^\pm(x)}{\partial B_k}$ exists only for $n = k$ or $n = k + 1$, but $\left\{ \frac{\partial L_{n\alpha}}{\partial B_k}, \frac{\partial M_{n\alpha}}{\partial B_k} \right\}$ are defined for all values of *n*.

<u>*Surface emission Jacobian*</u>. We make one remark here about Jacobians with respect to the surface Planck function B_{sur}. Clearly none of the particular integrals depend on this quantity, so there are no derivatives there; we are left with a linearization of the boundary value problem. If we write $\delta_{sur} = \partial / \partial B_{sur}$, the linearized problem is $\delta_{sur} \mathbb{V} = \mathbb{M}^{-1}. \delta_{sur} \mathbb{Y}$, where from Eq. (A1.6.11):

$$\delta_{sur} \mathbb{Y} = \begin{pmatrix} 0 \\ 0 \\ \ldots \\ 0 \\ \mathbb{E} \end{pmatrix}. \tag{A1.6.16}$$

A1.6.4 Temperature Profile Jacobians

Here we consider temperature dependence for both Planck functions and layer optical properties. We assume at the start that we have already obtained (1) profile Jacobian output from VLIDORT with respect to optical properties in *layers*, and (2) profile Jacobian output with respect to the Planck functions at *levels* - the new feature described in the previous sections. In addition, we assume that Planck function temperature derivatives $\{\partial B_n / \partial T_n\}$ are defined for $n = 0,1, \cdots N_L$ for level boundary temperatures $\{T_n\}$.

To obtain relationships between layer optical properties and $\{T_n\}$, we follow the prescription in [*Spurr and Christi*, 2014], assuming that: (i) Atmospheric quantities (pressure $\{p_n\}$, temperature $\{T_n\}$, height $\{h_n\}$, trace gas volume mixing ratios $\{v_n\}$, aerosol particle concentrations $\{\epsilon_n\}$) are defined at level boundaries; (ii) for $\{p_n\}, \{T_n\}$ and $\{h_n\}$, the atmosphere is in hydrostatic equilibrium, but only one of these quantities is independently defined; (iii) integration between levels is be done using simple trapezoidal summation, with $\{T_n\}$ and $\{h_n\}$ interpolating log-linearly with $\{p_n\}$, and constituent quantities $\{v_n\}$ and $\{\epsilon_n\}$ interpolating linearly with height; and (iv) the air density at level *n* follows the rule $\rho_n = \Gamma \frac{p_n}{T_n}$, where Γ is a constant related to density at STP.

We assume for now that there is no fine-layering scheme involved in the integration of the hydrostatic equation (there is no loss of generality in this assumption). In this case, the *layer* trace gas absorption optical thickness $A_n(\lambda_s)$ at wavelength (λ_s) is then

$$G_n(\lambda_s) = \tfrac{1}{2} d_n \left\{ \frac{v_n p_n \sigma_{s,n}(T_n)}{T_n} + \frac{v_{n-1} p_{n-1} \sigma_{s,n-1}(T_{n-1})}{T_{n-1}} \right\} \Gamma. \qquad \text{(A1.6.17)}$$

Here Γ is a constant, $d_n = h_{n-1} - h_n$ is the height separation, and the cross-sections $\sigma_{s,n}(T_n)$ are assumed to be known functions of temperature. (In the thermal regime, cross-sections are determined through line-by-line (LBL) calculations based on line-spectroscopy data sets; the derivation of LBL temperature derivatives of $\sigma_{s,n}(T_n)$ was discussed in [*Spurr and Christi*, 2014]). We define the Rayleigh scattering optical thickness $R_n(\lambda_s)$ in a similar way, treating the Rayleigh cross-section ς_s as independent of temperature:

$$R_n(\lambda_s) = \tfrac{1}{2} d_n \left\{ \frac{p_n}{T_n} + \frac{p_{n-1}}{T_{n-1}} \right\} \varsigma_s \Gamma. \qquad \text{(A1.6.18)}$$

The aerosol optical thickness (AOT) can be written down similarly in terms of the aerosol loading and the extinction cross-section, but we assume that these quantities are independent of temperature and pressure.

From Eqs. (A1.6.17) and (A1.6.18), we have the following partial derivatives for $k = n - 1$ or $k = n$:

$$\frac{\partial G_n(\lambda_s)}{\partial T_k} = \tfrac{1}{2} \Gamma d_n \frac{v_k p_k}{T_k} \left\{ \frac{\partial \sigma_{s,k}}{\partial T_k} - \frac{\sigma_{s,k}}{T_k} \right\}; \quad \frac{\partial R_n(\lambda_s)}{\partial T_k} = -\tfrac{1}{2} \Gamma d_n \frac{p_k \varsigma_s}{{T_k}^2}. \qquad \text{(A1.6.19)}$$

From VLIDORT, we now have optical property <u>*layer*</u> Jacobians $\frac{\partial I}{\partial G_n}$ and $\frac{\partial I}{\partial R_n}$ for $n = 1, \ldots N_d$, and Planck function <u>*level*</u> Jacobians (from the previous section) $\frac{\partial I}{\partial B_n}$ for $n = 0,1, \ldots N_d$. Then application of chain-rule derivatives yields the complete level-boundary temperature Jacobians, where we have written $j = k - 1$:

$$\frac{\partial I}{\partial T_k} = \frac{\partial I}{\partial B_k}\frac{\partial B_k}{\partial T_k} + \left\{ \frac{\partial I}{\partial G_k}\frac{\partial G_k}{\partial T_k} + \frac{\partial I}{\partial G_j}\frac{\partial G_j}{\partial T_k} \right\} + \left\{ \frac{\partial I}{\partial R_k}\frac{\partial R_k}{\partial T_k} + \frac{\partial I}{\partial R_j}\frac{\partial R_j}{\partial T_k} \right\} \quad k = 1, \cdots N-1; \qquad \text{(A1.6.20)}$$

$$\frac{\partial I}{\partial T_0} = \frac{\partial I}{\partial B_0}\frac{\partial B_0}{\partial T_0} + \frac{\partial I}{\partial G_1}\frac{\partial G_1}{\partial T_0} + \frac{\partial I}{\partial R_1}\frac{\partial R_1}{\partial T_0}; \qquad \text{(A1.6.21)}$$

$$\frac{\partial I}{\partial T_N} = \frac{\partial I}{\partial B_N}\frac{\partial B_N}{\partial T_N} + \frac{\partial I}{\partial G_N}\frac{\partial G_N}{\partial T_N} + \frac{\partial I}{\partial R_N}\frac{\partial R_N}{\partial T_N}. \qquad \text{(A1.6.22)}$$

These formulae may be readily generalized if there is fine-layer trapezoidal summation assumed in the hydrostatic equation integration - this was done for trace gas absorption and Rayleigh optical thickness values in [*Spurr and Christi*, 2014], and the results are equally applicable here.

The Planck Function temperature derivative is easy to write down. Indeed:

$$B(T) = \frac{2h\nu^3}{c^2}\frac{1}{e^{\frac{h\nu}{k_B T}}-1}, \tag{A1.6.23}$$

in terms of the usual constants h, c and k_B (Boltzmann's constant), and frequency ν. Thus

$$\frac{\partial B(T)}{\partial T} = \frac{2h\nu^3}{c^2}\frac{e^{\frac{h\nu}{k_B T}}}{\left(e^{\frac{h\nu}{k_B T}}-1\right)^2}\frac{h\nu}{k_B T^2}. \tag{A1.6.24}$$

In practice, we use the integrated form $2\Delta\upsilon\bar{B}_\nu(T) = \int_{\nu-\Delta\upsilon}^{\nu+\Delta\upsilon} B_\nu(T)d\nu$ over a small interval $2\Delta\upsilon$. This is done numerically, and the integration uses several numerical approximations depending on the wave-number region. The same approximations can be applied for the integrated form of the temperature derivative in Eq. (A1.6.5). Some software has been developed for VLIDORT to deliver Planck function T-derivatives, starting from the numerical routine supplied for the DISORT code [*Stamnes et al*., 2000].

A2. The Numerical VLIDORT Model

A2.1 Performance considerations

A2.1.1 BVP telescoping

For some Fourier component m, we consider a single active layer with non-trivial RTE solutions; all other atmospheric layers have no scattering (the extension to a number of *adjacent* active layers is easy). Vectors $\mathbf{L}_n$ and $\mathbf{M}_n$of Integration constants in layer n are given through

$$I^{\pm}(x,\mu_i) = \sum_{\alpha=1}^{N_d}\left[L_{n\alpha}X_{in\alpha}^{\pm}e^{-k_{n\alpha}x} + M_{n\alpha}X_{in\alpha}^{\mp}e^{-k_{n\alpha}(\Delta_n - x)}\right] + G_{in}^{\pm}e^{-x/\mu_0}. \qquad \text{(A2.1.1)}$$

Here, $\mathbf{X}_{n\alpha}$ and $k_{n\alpha}$ denote the homogeneous solution vectors and separation constants respectively, $\mathbf{G}_n$ is the solar source vectors (a plane-parallel solution has been assumed). The boundary value problem (BVP) for the entire atmosphere is posed by compiling boundary conditions *at all levels* to create a large sparse linear algebra system. The BVP matrix has size $2N_dN_L$, where N_L is the total number of layers, and although there are band compression algorithms in place to aid with the LU-decomposition and inversion of this matrix, the BVP solution step is the most expensive CPU process in the LIDORT code.

Let us assume that n is an "active" layer with scattering particles in what is otherwise a non-scattering Rayleigh atmosphere. Then we have $X_{ip\alpha}^{\pm} = \delta_{i\alpha}$ and $G_{ip}^{\pm} = 0$ for all Fourier $m > 2$ and for all layers $p \neq n$. In this case the downwelling and upwelling solutions are:

$$I_{pj}^{\downarrow}(x) = L_{pj}\exp[-x/\mu_j]; \qquad \text{(A2.1.2a)}$$

$$I_{pj}^{\uparrow}(x) = M_{pj}\exp[-(\Delta_p - x)/\mu_j]. \qquad \text{(A2.1.2b)}$$

Boundary value constants will clearly propagate upwards and downwards through all these non-scattering layers via:

$$L_{p+1,j} = L_{pj}\exp[-\Delta_p/\mu_j]; \qquad \text{(A2.1.3a)}$$

$$M_{p-1,j} = M_{pj}\exp[-\Delta_p/\mu_j]. \qquad \text{(A2.1.3b)}$$

If we can find BVP integration constants $\mathbf{L}_n$ and $\mathbf{M}_n$ for the active layer n, then coefficients for all other layers will follow by propagation. We now write down the boundary conditions for layer n. At the top of the active layer, we have:

$$\sum_{\alpha=1}^{N_d}[L_{n\alpha}X_{in\alpha}^{+} + M_{n\alpha}X_{in\alpha}^{-}\Theta_{n\alpha}] + G_{in}^{+} = L_{n-1,i}C_{n-1,i}; \qquad \text{(A2.1.4a)}$$

$$\sum_{\alpha=1}^{N_d}[L_{n\alpha}X_{in\alpha}^{-} + M_{n\alpha}X_{in\alpha}^{+}\Theta_{n\alpha}] + G_{in}^{-} = M_{n-1,i}. \qquad \text{(A2.1.4b)}$$

At the bottom of the active layer, we have

$$\sum_{\alpha=1}^{N_d}[L_{n\alpha}X_{in\alpha}^{+}\Theta_{n\alpha} + M_{n\alpha}X_{in\alpha}^{-}] + G_{in}^{+}\Lambda_{n\alpha} = L_{n+1,i}; \qquad \text{(A2.1.5a)}$$

$$\sum_{\alpha=1}^{N_d}[L_{n\alpha}X_{in\alpha}^{-}\Theta_{n\alpha} + M_{n\alpha}X_{in\alpha}^{+}] + G_{in}^{-}\Lambda_{n\alpha} = M_{n+1,i}\,C_{n+1,i}. \qquad \text{(A2.1.5b)}$$

We have used the following abbreviations:

$$\Theta_{n\alpha} = \exp[-k_{n\alpha}\Delta_n], \quad \Lambda_{n\alpha} = \exp[-\eta_n\Delta_n], \quad C_{nj} = \exp[{}^{-\Delta_n}/_{\mu_j}]. \qquad \text{(A2.1.6)}$$

We now consider the upper and lower boundary conditions. At TOA, there is no diffuse radiation, so that $\mathbf{L}_p = 0$ for $p = 1$ and hence by Eq. (A2.1.2a) also for all $p < n$. At BOA, the Lambertian reflection condition only applies to Fourier $m = 0$, and for all other components there is no reflection, and so in our case $\mathbf{M}_p = 0$ for $p = N_L$ and hence by Eq. (A2.1.2b) also for all $p > n$. With these conditions, Eqs. (A2.1.4a) and (A2.1.5b) become:

$$\sum_{\alpha=1}^{N_d}[L_{n\alpha}X_{in\alpha}^{+} + M_{n\alpha}X_{in\alpha}^{-}\Theta_{n\alpha}] = -G_{in}^{+}; \qquad \text{(A2.1.7a)}$$

$$\sum_{\alpha=1}^{N_d}[L_{n\alpha}X_{in\alpha}^{-}\Theta_{n\alpha} + M_{n\alpha}X_{in\alpha}^{+}] = -G_{in}^{-}\Lambda_{n\alpha}. \qquad \text{(A2.1.7b)}$$

For this single layer, we then have a linear system of rank $2N_d$ for the desired unknowns $\mathbf{L}_n$ and $\mathbf{M}_n$ (there is actually no band-matrix compression for a single layer). For the layer immediately above n, we use (A2.1.4b) to find $\mathbf{M}_{n-1}$ and for remaining layers to TOA we use (A2.1.3b). Similarly for the layer immediately below n, we use (A2.1.5a) to find $\mathbf{L}_{n+1}$ and for remaining layers to BOA, we use (A2.1.3a). This completes the BVP telescoping process.

If the telescoped BVP is written as $\mathbb{A} * \mathbb{Y} = \mathbb{B}$, then the corresponding linearized problem may be written $\mathbb{A} * \mathcal{L}_k(\mathbb{Y}) = \mathbb{B}' \equiv \mathcal{L}_k(\mathbb{B}) - \mathcal{L}_k(\mathbb{A}) * \mathbb{Y}$; the k subscript refers to the layer for which weighting functions are required. The latter is essentially the same problem with a different source vector, and the solution may be found be back-substitution, since the matrix inverse $\mathbb{A}^{-1}$ is already known from the original BVP solution. Construction of the source vector $\mathbb{B}'$ depends on the RTE solution linearizations; clearly if $k = n$ there will be more contributions to consider than if $k < n$. However the linearized boundary conditions for $\mathbb{B}'$ are essentially the same as those noted for the full atmosphere problem – the only thing to remember is that the upper boundary is the same as TOA but with the first layer active, and the lower boundary is the same as BOA but with the last layer active.

NOTE (Version 2.4): The above treatment allowed for telescoping to be done for a single active scattering layer in the atmosphere; this has been generalized in VLIDORT Versions 2.4 and higher to allow telescoping for any contiguous set of active scattering layers. This generalization also applies to the scalar LIDORT code (Version 3.3 and higher).

A2.2 Taylor series expansions in VLIDORT

We now turn to the use of Taylor series expansions for situations where numerical instability may be present in solutions of the RTE. In particular we consider several "multipliers" which occur in the RT derivation of whole-layer solutions to various components of the RT field. These multipliers arise from optical-thickness integrations of solutions of the homogeneous RTE, layer solutions of the single-scattering field, and layer solutions of the diffuse source term field (the latter derived through Green's function methods in LIDORT).

The first two multipliers occur in both LIDORT and VLIDORT, but at the present time, only the scalar model LIDORT has a complete Green's function RTE solution for diffuse-field source terms. Although in general, VLIDORT solves the particular integral RTE using a substitution method, the Green's function formulation has been applied to the solution of the azimuth-independent vector RTE in a medium with Rayleigh scattering only.

A2.2.1 Multipliers for the intensity field

We first look at the homogeneous-solution and primary-scatter *downwelling* multipliers, and the Green's function (downwelling) multiplier for the diffuse source term at discrete-ordinate polar cosines. These are respectively:

$$H_j^{\downarrow} = \frac{(e^{-\Delta k_j} - e^{-\Delta\mu^{-1}})}{\mu^{-1} - k_j};\; F^{\downarrow} = \frac{(e^{-\Delta\mu^{-1}} - e^{-\Delta\lambda})}{\lambda - \mu^{-1}};\; G_j^{\downarrow} = \frac{(e^{-\Delta k_j} - e^{-\Delta\lambda})}{\lambda - k_j}. \quad \text{(A2.2.1)}$$

Here, λ is the layer average secant corresponding to spherical-atmosphere attenuation of a solar beam with solar zenith angle cosine μ_0 ($\lambda = 1/\mu_0$ in plane-parallel attenuation), k_j is the separation constant corresponding to discrete ordinate stream *j* arising from solution of the homogeneous RTE eigenproblem, μ is the cosine of the line-of sight viewing polar angle, and Δ is the layer total optical depth. [Layer index n is suppressed for clarity].

Remark. For polarized RT with VLIDORT, some of the separation constants k_j may be complex variables; λ and μ are always real-valued. Taylor series expansions involving k_j are only applicable for real values of this quantity.

We consider the limiting cases $|\lambda - k_j| \to 0$, $|\mu^{-1} - k_j| \to 0$ or $|\lambda - \mu^{-1}| \to 0$. Writing ϵ for any of these quantities, if the order of the Taylor-series expansion is M, then we neglect terms $O(\epsilon^{M+1})$. Considering first the multiplier $G_j^{\downarrow}$ from Eq. (A2.2.1), then if $\epsilon = \lambda - k_j$, we have $e^{-\Delta k_j} = We^{\epsilon\Delta} \approx W\mathbf{z}_{M+1}(\Delta)$, where we have written $W = e^{-\Delta\lambda}$ for convenience, and we have used the notation $\mathbf{z}_{M+1}(x) = \sum_{m=0}^{M+1} z_m(x)\epsilon^m$ to approximate the exponential $e^{\epsilon\Delta}$, so that the coefficients are $z_0(x) = 1, z_m(x) = x^m/m!$ for $0 < m \leq M+1$. Applying the expansion, we find:

$$G_j^{\downarrow} \approx \frac{W(\mathbf{z}_{M+1}(\Delta) - 1)}{\epsilon} = \Delta W \mathbf{z}_M^*(\Delta). \quad \text{(A2.2.2)}$$

Here, the new coefficients are $z_0^* = 1, z_m^* = \Delta^m/(m+1)!$ for $0 < m \leq M$. Note that we need to expand first to order $M+1$ to ensure that the final expression is defined to order M.

We continue to use this notation in the sequel. Next we look at those two multipliers for the Green's function post-processed field which may be susceptible to instability through use of the difference $\lambda - k_j$ appearing in the denominator. From the theory [*Spurr*, 2002] (see also Chapter 2), these multipliers are:

$$M_j^{\uparrow\uparrow} = \frac{H_j^{\uparrow} - F^{\uparrow}}{\lambda - k_j};\quad M_j^{\downarrow\downarrow} = \frac{H_j^{\downarrow} - F^{\downarrow}}{\lambda - k_j}, \quad \text{(A2.2.3)}$$

where $H_j^{\downarrow}$ and $F^{\downarrow}$ have been defined in Eq. (A2.2.1), and

$$H_j^{\uparrow} = \frac{(1 - e^{-\Delta k_j} e^{-\Delta\mu^{-1}})}{\mu^{-1} + k_j};\; F^{\uparrow} = \frac{(1 - e^{-\Delta\mu^{-1}} e^{-\Delta\lambda})}{\lambda + \mu^{-1}}. \quad \text{(A2.2.4)}$$

Looking at $M_j^{\uparrow\uparrow}$ in Eq. (A2.2.3), we set $k_j = \lambda - \epsilon$, and find

$$M_j^{\uparrow\uparrow} \approx \frac{Y}{\epsilon}\left[\left(1 - WU\mathbf{z}_{M+1}(\Delta)\right)\mathbf{a}_{M+1}(Y) - (1 - WU)\right], \quad \text{(A2.2.5)}$$

where $U = e^{-\Delta\mu^{-1}}$, $Y = (\lambda + \mu^{-1})^{-1}$, and series $\mathbf{a}_{M+1}(x)$ has coefficients $a_0(x) = 1$, $a_m(x) = x^m$ for $0 < m \leq M+1$. Since $a_0 = z_0 = 1$, it is apparent that the $(1 - WU)$ contributions will fall out, and the result can then be written:

$$M_j^{\uparrow\uparrow} \approx Y[Y\mathbf{a}_M(Y) - WU\mathbf{c}_M(\Delta, Y)]. \qquad \text{(A2.2.6)}$$

Here $\mathbf{c}_M(\Delta, Y)$ has coefficients $c_0 = 1$, and $c_m(\Delta, Y) = \sum_{p=0}^{m} z_p(\Delta) a_{m-p}(Y)$ for $0 < m \leq M$. We have found that use of these series coefficients is convenient for computation, allowing us to generate expressions to any order of accuracy without complicated algebraic expressions.

The other multiplier $M_j^{\downarrow\downarrow}$ in Eq. (A2.2.3) may be treated similarly. Note that multipliers in Eq. (A2.2.4) are stable entities, along with the other Green's function multipliers $G_j^{\uparrow}$, $M_j^{\downarrow\uparrow}$ and $M_j^{\uparrow\downarrow}$, the latter three quantities being defined with denominator $\lambda + k_j$.

These multipliers are required for output of the upwelling and downwelling radiance fields at layer boundaries. VLIDORT has the ability to generate output at any level away from layer boundaries (the "partial-layer" option). In this case, source function integration to an optical thickness $\tau < \Delta$ in layer n will result in "partial-layer" multipliers similar to those already defined here. For example,

$$H_j^{\downarrow}(\tau) = \frac{\left(e^{-\tau k_j} - e^{-\tau\mu^{-1}}\right)}{\mu^{-1} - k_j};\ F^{\downarrow}(\tau) = \frac{\left(e^{-\tau\mu^{-1}} - e^{-\tau\lambda}\right)}{\lambda - \mu^{-1}};\ G_j^{\downarrow}(\tau) = \frac{\left(e^{-\tau k_j} - e^{-\tau\lambda}\right)}{\lambda - k_j}, \qquad \text{(A2.2.7)}$$

are the downwelling partial-layer multipliers equivalent to those in Eq. (A2.2.1). Taylor series expansions for these and the corresponding Green's function multipliers have been generated in a similar fashion.

A2.2.2 Linearized Multipliers

VLIDORT is a linearized RT model with the ability to generate analytically both profile and total-column Jacobians with respect to any atmospheric quantity. The entire discrete ordinate solution is analytically differentiable [*Spurr*, 2002] with respect to these variables, and this includes the multipliers discussed above. It is therefore necessary to develop Taylor series expansions for those *linearized* multipliers which are susceptible to instability as noted above.

We assume the choice of layer n is given. We start with partial derivatives $\dot{k}_j \equiv \partial k_j/\partial\xi$, $\dot{\lambda} \equiv \partial\lambda/\partial\xi$ and $\dot{\Delta} \equiv \partial\Delta/\partial\xi$ with respect to some atmospheric quantity ξ. Since the layer optical depth Δ is an intrinsic optical property (input to VLIDORT), its derivative is also an intrinsic input. The viewing angle cosine μ has no derivative. Note that $\dot{k}_j = 0$ and $\dot{\Delta} = 0$ for a <u>*profile*</u> atmospheric quantity ξ_m defined in layer $m \neq n$ (no cross-layer derivatives); on the other hand, the average secant λ will have cross-layer derivatives for layers $m < n$, thanks to solar beam attenuation through the atmosphere. Considering the third multiplier in Eq. (A2.2.1), its derivative is

$$\frac{\partial G_j^{\downarrow}}{\partial\xi} = \frac{-e^{-\Delta k_j}\left(\dot{k}_j\Delta + k_j\dot{\Delta}\right) + e^{-\Delta\lambda}\left(\dot{\lambda}\Delta + \lambda\dot{\Delta}\right) - G_j^{\downarrow}(\dot{\lambda} - \dot{k}_j)}{\lambda - k_j}. \qquad \text{(A2.2.8)}$$

Expanding Eq. (A2.2.8) as a Taylor series with $k_j = \lambda - \epsilon$, and using the series-coefficient notation developed in the previous section, we find:

$$\frac{\partial G_j^{\downarrow}}{\partial \xi} \approx \frac{-(\dot{k}_j\Delta+\lambda\dot{\Delta}+\epsilon\dot{\Delta})W\mathbf{z}_{M+1}+(\dot{\lambda}\Delta+\lambda\dot{\Delta})W-(\dot{\lambda}-\dot{k}_j)\Delta W\mathbf{z}^*_{M+1}}{\epsilon}. \tag{A2.2.9}$$

Again, $W = e^{-\Delta\lambda}$, and the series $\mathbf{z}_{M+1}$ and $\mathbf{z}^*_{M+1}$ have argument Δ and were defined in the previous section. Since $z_0 = z_0^* = 1$, the lowest-order terms in the numerator of Eq. (A2.2.9) will fall out, and we are left with:

$$\frac{\partial G_j^{\downarrow}}{\partial \xi} \approx -W\left[\dot{\Delta}\mathbf{z}_M + \left(\dot{k}_j\Delta + \lambda\dot{\Delta}\right)\Delta\mathbf{z}^*_M + (\dot{\lambda} - \dot{k}_j)\Delta^2\mathbf{z}^{\dagger}_M\right], \tag{A2.2.10}$$

where the third series $\mathbf{z}^{\dagger}_M$ has coefficients $z^{\dagger}_0 = 1/2$ and $z^{\dagger}_m = \Delta^m/(m+2)!$ for $0 < m \leq M$. Note that the presence of the series $\mathbf{z}^{\dagger}_M$ to order M implies that the original series must be computed to order $M+2$, that is, we require $\mathbf{z}_{M+2}$.

Linearization of the Green's function multipliers in Eq. (A2.2.3) follows similar considerations. We give one example; explicit differentiation of $M_j^{\uparrow\uparrow}$ yields

$$\frac{\partial M_j^{\uparrow\uparrow}}{\partial \xi} = \frac{\dot{H}_j^{\uparrow} - \dot{F}^{\uparrow} - (\dot{\lambda}-\dot{k}_j)M_j^{\uparrow\uparrow}}{\lambda - k_j}; \tag{A2.2.11}$$

with

$$\dot{H}_j^{\uparrow} = \frac{Ue^{-\Delta k_j}[\dot{\Delta}(\mu^{-1}+k_j)+\dot{k}_j\Delta]-\dot{k}_jH_j^{\uparrow}}{\mu^{-1}+k_j}; \tag{A2.2.12}$$

$$\dot{F}^{\uparrow} = \frac{UW[\dot{\Delta}(\mu^{-1}+\lambda)+\dot{\lambda}\Delta]-\dot{\lambda}F^{\uparrow}}{\lambda+\mu^{-1}}. \tag{A2.2.13}$$

Expanding in the usual manner and employing results established already, we find

$$\dot{H}_j^{\uparrow} \approx \left[UW\left(\dot{k}_j\Delta + \dot{\Delta}Y^{-1} - \epsilon\dot{\Delta}\right)\mathbf{z}_N - \dot{k}_jY(1 - WU\mathbf{z}_N)\mathbf{a}_N\right]Y\mathbf{a}_N; \tag{A2.2.14}$$

$$\dot{F}^{\uparrow} = \left[UW\left(\dot{\lambda}\Delta + \dot{\Delta}Y^{-1}\right) - \dot{\lambda}Y(1 - WU)\right]Y, \tag{A2.2.15}$$

where now $N = M+2$ terms in the series have been retained in the expansions. Eq. (A2.2.11) implies that we also require the original multiplier $M_j^{\uparrow\uparrow}$ expanded to order $M+1$, that is,

$$M_j^{\uparrow\uparrow} \approx Y[Y\mathbf{a}_{M+1}(Y) - WU\mathbf{c}_{M+1}(\Delta, Y)], \tag{A2.2.16}$$

should be used in Eq. (A2.2.11). Putting together the above three equations, and canceling out the lowest-order terms in the expansions, we find after some algebra that

$$\frac{\partial M_j^{\uparrow\uparrow}}{\partial \xi} \approx Y\left[WU\mathbf{S}_M^{(1)} - \mathbf{S}_M^{(2)} - \mathbf{S}_M^{(3)}\right], \tag{A2.2.17}$$

where the three series $\mathbf{S}_M^{(q)} = \sum_{m=0}^{M} s_m^{(q)}\epsilon^m$ have coefficients

$$s_m^{(1)} = \left(\dot{\Delta}Y^{-1} + \dot{k}_j\Delta\right)c_{m+1}(\Delta, Y) - \dot{\Delta}c_m(\Delta, Y); \tag{A2.2.18}$$

$$s_m^{(2)} = Y\dot{k}_j[b_{m+1}(Y) + WUd_{m+1}(\Delta, Y)]; \tag{A2.2.19}$$

$$s_m^{(3)} = \left(\dot{\lambda} - \dot{k}_j\right)[b_{m+2}(Y) + WUc_{m+2}(\Delta, Y)]. \tag{A2.2.20}$$

Subsidiary coefficients for $0 < m \leq M$ are given by $a_m = Y^m$ (series expansion of $(1 - \epsilon Y)^{-1}$), and $b_m = (m+1)Y^m$ (series expansion of $(1 - \epsilon Y)^{-2}$). We also have the product coefficients $c_m(\Delta, Y) = \sum_{p=0}^{m} z_p(\Delta) a_{m-p}(Y)$ and $d_m(\Delta, Y) = \sum_{p=0}^{m} z_p(\Delta) b_{m-p}(Y)$ obtained from the first exponential series $\mathbf{z}(\Delta)$ which approximates $e^{\Delta\epsilon}$.

Derivatives of the other multipliers subject to possible instability may be obtained similarly, and there are also derivatives of the partial-layer multipliers to be considered.

Software for all these instability cases has been compiled in two new modules (`lidort_Taylor.f90` and `vlidort_Taylor.f90` in the respective RT models) - in each case, the order M controls the accuracy of the Taylor series expansions. The other parameter controlling the use of these limiting-case calculations is the "small-number" value ϵ. VLIDORT uses double-precision floating-point arithmetic. With this in mind, we have chosen $\epsilon = 10^{-3}$ as the default, after testing linearized multiplier accuracies obtained by running the model with and without the instability corrections. In practice $M = 3$ provides more than sufficient accuracy for this choice of ϵ.

A3. Kernels in VLIDORT VBRDF Supplement

A3.1 Ocean glitter kernels

A3.1.1 Cox-Munk Glint reflectance

For ocean glitter, we use the well-known geometric-optics regime for a single rough-surface redistribution of incident light, in which the reflection function is governed by Fresnel reflectance and takes the form [*Jin et al.*, 2006]:

$$\rho_{CM}(\mu,\mu',\varphi-\varphi',m,\sigma^2) = \frac{F(m,\theta_r)}{\mu\mu'|\gamma_r|^4}P(\gamma_r,\sigma^2)D(\mu,\mu',\sigma^2) \qquad \text{(A3.1.1)}$$

Here, σ^2 is the slope-squared variance (also known as the mean-slope-square) of the Gaussian probability function $P(\gamma_r,\sigma^2)$ which has argument γ_r (the polar direction of the reflected beam), $D(\mu,\mu',\sigma^2)$ is a shadow function correction [*Sancer*, 1969].

$F(m,\theta_r)$ is the scalar Fresnel reflection for incident angle $\theta_r = \frac{1}{2}\theta_{SCAT}$ and relative refractive index m. The scattering angle θ_{SCAT} is determined in the usual manner from the incident and reflected directional cosines μ' and μ, and the relative azimuth $\varphi-\varphi'$.

The two non-linear parameters characterizing this kernel are $\{m,\sigma^2\}$. The probability and shadow functions are given by:

$$P(\alpha,\sigma^2) = \frac{1}{\pi\sigma^2}\exp\left[-\frac{\alpha^2}{\sigma^2(1-\alpha^2)}\right]; \quad D(\alpha,\beta,\sigma^2) = \frac{1}{1+\Lambda(\alpha,\sigma^2)+\Lambda(\beta,\sigma^2)};$$

$$\Lambda(\alpha,\sigma^2) = \frac{1}{2}\left\{\sqrt{\frac{(1-\alpha^2)}{\pi}}\frac{\sigma}{\alpha}\exp\left[-\frac{\alpha^2}{\sigma^2(1-\alpha^2)}\right] - erfc\left[-\frac{\alpha}{\sigma\sqrt{(1-\alpha^2)}}\right]\right\}. \qquad \text{(A3.1.2)}$$

The variance is commonly related to the wind speed W in (m/s) through the empirical relation $\sigma^2 = 0.003 + 0.00512W$ [*Cox and Munk*, 1954]. A typical value for m is 1.33.

For the linearization, the key parameter is the wind-speed (or equivalently, the mean slope-square) The probability function is easily differentiated with respect to σ^2. Indeed, we have:

$$\frac{\partial P(\alpha,\sigma^2)}{\partial\sigma^2} = \frac{P(\alpha,\sigma^2)}{\sigma^4}\left[\frac{\alpha^2}{(1-\alpha^2)} - \sigma^2\right]. \qquad \text{(A3.1.3)}$$

Again, the shadow function can be differentiated analytically with respect to σ^2 in a straightforward manner, once we recall that the derivative of the error function is Gaussian. We thus have linearized BRDF quantities prepared for (V)LIDORT, which will then be able to generate *analytic weighting functions with respect to the wind speed*.

Linearization of the kernel with respect to refractive index *m* will require the partial derivative $\partial F(m,\theta_r)/\partial m$, which is easy to determine from the usual Fresnel formula; this Jacobian is less useful.

We note also that VLIDORT has a vector kernel function for sea-surface glitter reflectance, based on the specification in [*Mishchenko and Travis*, 1997]. This is called the "GISS Cox-Munk" kernel in the VLIDORT code.

This formulation is for a single Fresnel reflectance by wave facets. In reality, glitter is the result of many reflectances. It is possible to incorporate a correction for multiple reflectances for this glitter contribution, both for the direct-bounce term and the Fourier components. Given that the glitter maximum is typically dominated by direct reflectance of the solar beam, we confine discussion to multiple-reflectance of this term. We consider only one extra order of reflectance:

$$R(\Omega,\Omega_0) \cong R_0(\Omega,\Omega_0) + R_1(\Omega,\Omega_0);\;\; R_1(\Omega,\Omega_0) = \int_0^{2\pi}\int_0^1 R_0(\Omega,\Omega')R_0(\Omega',\Omega_0)d\mu' d\varphi'. \tag{A3.1.4}$$

$R_0(\Omega,\Omega')$ is the zeroth-order reflectance from incident direction $\Omega' = \{\mu',\varphi'\}$ to reflected direction $\Omega = \{\mu,\varphi\}$. The azimuthal integration is done by double Gaussian quadrature over the intervals $[-\pi,0]$ and $[0,\pi]$; the polar stream integration is also done by quadrature. It is obviously possible to calculate higher orders of reflectance for all BRDF functions, but this rapidly becomes computationally prohibitive. We have found that the neglect of multiple glitter reflectances can lead to errors of 1-3% in the upwelling intensity at the top of the atmosphere, the higher figures being for larger solar zenith angles. Finally, we note that the higher-order reflectances are in turn differentiable with respect to the slope-squared parameter, so that Jacobians for the wind speed can still be determined.

A3.1.2 Alternative Cox-Munk Glint reflectance

The above ocean-glint reflectance option in VLIDORT is based on an older implementation of the well-known Cox-Munk distribution of wave facets - this does not include any treatment of whitecaps (foam), and there is no allowance for the wind direction. Further, the CM implementation is based on a fixed real-valued refractive index for water.

We have now added an alternative Cox-Munk implementation which addresses these issues. This new-CM option is based on the glint treatment in the 6S code [*Vermote et al*., 1997; *Kotchenova et al*., 2006], and includes an empirical whitecap contribution. The latter model also includes a more recent treatment of water-leaving radiance [*Morel and Gentili*, 2009], and the LIDORT SLEAVE supplement has been updated according to the 6S treatment. These new 6S-based options in the VLIDORT BRDF and SLEAVE supplements are designed to operate in tandem. Indeed, the total surface radiance in the 6S model is given by

$$I(\mu_1,\mu_0,\varphi_1-\varphi_0) = (1-R_{wc})S(\mu_1,\mu_0) + R_{wc} + (1-R_L)\,\rho_{NCM}(\mu_1,\mu_0,\varphi_1-\varphi_0), \tag{A3.1.5}$$

where the water-leaving term $S(\mu_1,\mu_0)$ does depend on the outgoing and incoming directions but is azimuth-independent, ρ_{NCM} is the Cox-Munk glint reflectance, and R_{wc} and R_L are the empirically-derived whitecap contributions (final and Lambertian).

For VLIDORT to possess this functionality for the ocean surface, the BRDF supplement must provide the second and third terms on the right-hand-side of (A3.1.5), while the SLEAVE supplement supplies the first term. Note that both supplements require the same whitecap formulation. The derivation of the water-leaving term is done in the next section.

The Cox-Munk calculation for ρ_{NCM} depends on the wind speed, wind-direction and refractive index. The latter is a complex variable that depends on the salinity of the ocean, and we use the 6S formulation. The anisotropic treatment assumes an (azimuthal) wind direction relative to the solar incident beam, and this follows the formulae developed by Cox and Munk in the 1950s.

For facet anisotropy, the wind-direction is dependent on the solar position, and it follows that any BRDF quantity will pick up additional dependence on the solar angle. It is then only possible to use this "New-CM" option with a single solar zenith angle (and hence a single wind-direction azimuth) - multiple solar beams are ruled out. See also the remark in section 5.3.6 in the Main Guide regarding use of the black-sky albedo. There is exception handling for this eventuality.

In addition, we have linearized this "New-CM" glint reflectance with respect to the wind speed. Finally, we note that the surface-leaving contribution to the glint reflectance is scalar only, so that the above considerations apply only to the (1,1) element of this contribution (Polarization of this contribution is currently undergoing investigation).

A3.2 Land-surface BRDF kernels

A3.2.1 MODIS BRDF system

The five MODIS-type kernels (numbers 2-5 and 7 in Table 5.3.1 of the Main guide) [*Wanner et al*., 1995] must be used in a linear combination with a Lambertian kernel. The kernels divide naturally into two groups: the *volume scattering* terms with no non-linear parameters (Ross-thin, Ross-thick) and the *geometric-optics* terms with 2 non-linear parameters (Li-sparse, Li-dense) or no non-linear parameters (Roujean). See [*Wanner et al*., 1995] and [*Spurr*, 2004] for details of the kernel formulae.

In fact, it is standard practice in MODIS BRDF retrievals to use a combination of Lambertian, Ross-thick and Li-Sparse kernels, and this 3-kernel combination is common

$$\rho_{total}(\Omega,\Omega') = f_{iso} + f_{vol}\rho_{RossThick}(\Omega,\Omega') + f_{geo}\rho_{LiSparse}(\Omega,\Omega') \qquad \text{(A3.2.1)}$$

An alternative form of the Ross kernels has also been introduced – this has a better parameterization of the hot-spot effect. The Rahman and Hapke kernels (6 and 8 in Table 5.3.1 of the Main guide)were discussed in [R1].

A3.2.2 BPDF Kernels

The 3 BPDF kernels [*Maignan et al*., 2009] (12-14 in Table 5.3.1 in the Main guide) were developed as semi-empirical models for polarized land-surface bidirectional reflectances. All three kernels are based on Fresnel reflectance. The polarization effects enter through the Fresnel reflectance term; for LIDORT, we require only the scalar Fresnel reflectance.

For the BPDF "Soil" type, the scalar reflectance is:

$$\rho_{SOIL}(\mu,\mu',\varphi-\varphi',m) = \frac{F(m,\theta_r)}{4\mu\mu'}(1-\sin\theta_r). \qquad \text{(A3.2.2)}$$

As before, $F(m,\theta_r)$ is the Fresnel reflection for incident angle $\theta_r = \frac{1}{2}\theta_{SCAT}$ and relative refractive index m (which is the sole kernel parameter). Linearization of the kernel with respect to refractive index *m* requires the partial derivative of $F(m,\theta_r)$.

For the BDPF "Vegetation" type, there is dependence on the leaf orientation probability $\sigma(\alpha)$ and the leaf facet projections, through use of a plagiophile distribution:

$$\rho_{VEGN}(\mu,\mu',\varphi-\varphi',m) = \frac{F(m,\theta_r)}{4\mu\mu'}\frac{\zeta(\alpha)}{\mathrm{H}}(1-\sin\theta_r); \qquad \text{(A3.2.3)}$$

$$\zeta(\alpha) = \frac{16}{\pi}\cos^2\alpha \sin\alpha\,; \quad \cos\alpha = \frac{(\mu+\mu')}{2\cos\theta_r};$$

$$\mathrm{H} = \frac{\sum_{k=0}^{3} a_k \mu^k}{\mu} + \frac{\sum_{k=0}^{3} a_k \mu'^k}{\mu'},$$

where the leaf projection H depends on the set of "plagiophile coefficients" $\{a_k\}$. Again, the refractive index is the only surviving kernel parameter to be considered for linearization.

For the BPDF "NDVI" kernel, we have:

$$\rho_{NDVI}(\mu, \mu', \varphi - \varphi', m, N, C) = \frac{CF(m,\theta_r)}{4(\mu+\mu')} \exp[-\tan\theta_r] \exp[-N], \qquad \text{(A3.2.4)}$$

where there are exponential attenuation terms, one of which depends on the NDVI N; in this formula, the scaling factor is C (nominally, this is set to 1.0). Linearizations with respect to the parameters N and C are easy to establish. The NDVI varies from -1 to 1 and is defined as the ratio of the difference to the sum of two radiance measurements, one in the visible and one in the infrared.

A3.2.3 Polarized land surface BRDF kernels

In general, BPDFs are "spectrally neutral", and modeling using specular reflection has become the accepted way of generating these functions. An empirical model was developed in part from specular reflection and in part from an analysis of POLDER measurements [*Nadal and Bréon*, 1999]. Recently, a great deal more BPDF information has been gleaned from data analysis of several years of measurements from the PARASOL instrument. Based on this analysis, the paper of [*Maignan et al.*, 2009] gives the following empirical formula for the BPDF:

$$\mathbf{Rp}_{NDVI}(\mu_i, \mu_j, \varphi_i - \varphi_j) = \frac{C\mathbf{Fp}(m,\theta_R)}{4(\mu_i+\mu_j)} \exp[-\tan\theta_R] \exp[-NDVI]. \qquad \text{(A3.2.5)}$$

Here, $\theta_R = \frac{1}{2}\theta_{SCAT}$, and vector Fresnel reflectance $\mathbf{Fp}(m, \theta_R)$ depends only on θ_R and refractive index m. The scattering angle θ_{SCAT} is determined in the usual manner from the incident and reflected directional cosines μ_i and μ_j, and the relative azimuth $\varphi_i - \varphi_j$. Calculation of **Fp** follows the specification given above for the GISS Cox-Munk BRDF. There are exponential attenuation terms, one of which depends on the NDVI Vegetation Index; in this formula, the scaling factor is C (nominally, this is set to 1.0).

There are three parameters characterizing the reflectance - the refractive index *m*, the Vegetation Index $NDVI$, and the scaling factor C. The $NDVI$ varies from -1 to 1 and is defined as the ratio of the difference to the sum of two radiance measurements, one in the visible and one in the infrared. Linearization of the kernel with respect to refractive index *m* will require the partial derivatives $\partial\mathbf{Fp}(m, \theta_R)/\partial m$, which are easy to determine from the Fresnel formulation. Linearizations with respect to the parameters $NDVI$ and C are easy to establish. Equation (A3.2.5) is the BPDF "NDVI" kernel.

The other BPDF kernels are defined similarly. For the "Soil" type, we have

$$\mathbf{Rp}_{SOIL}(\mu_i, \mu_j, \varphi_i - \varphi_j) = \frac{\mathbf{Fp}(m,\theta_R)}{4\mu_i\mu_j}(1 - \sin\theta_R). \qquad \text{(A3.2.6)}$$

Here, $\theta_R = \frac{1}{2}\theta_{SCAT}$ as before, and the refractive index m is the only parameter.

For the BDPF "Vegetation" type, there is dependence on the leaf orientation probability $\sigma(\alpha)$ and the leaf facet projections, through use of a plagiophile distribution:

$$\mathbf{Rp}_{VEGN}(\mu_i, \mu_j, \varphi_i - \varphi_j) = \frac{\mathbf{Fp}(m,\theta_R)}{4\mu_i\mu_j}\frac{\sigma(\alpha)}{P}(1 - \sin\theta_R); \qquad \text{(A3.2.6)}$$

$$\sigma(\alpha) = \frac{16}{\pi}\cos^2\alpha \sin\alpha\,; \quad \cos\alpha = \frac{(\mu_i + \mu_j)}{2\cos\theta_R};$$

$$P = \frac{\sum_{k=0}^{3} a_k \mu_i^k}{\mu_i} + \frac{\sum_{k=0}^{3} a_k \mu_j^k}{\mu_j},$$

where the leaf projection P depends on the set of "plagiophile coefficients" $\{a_k\}$. Again, the refractive index is the only surviving kernel parameter to be considered for linearization.

A4. Water-Leaving in VSLEAVE Supplement

A4.1 Ocean optics model

Much of the ocean optics model is based on the work of [*Sayer et al*., 2010], and the authors are indebted to Andrew Sayer for close review of this material.

We start first with pure water optical properties (wavelength λ is in Microns unless otherwise stated). The water absorption $\alpha_W(\lambda)$ is linearly interpolated from a table of values at every 5 nm from 200-900 nm. This table is patched together from a number of literature sources. These are (1) 200-320 nm [*Quickenden and Irvin*, 1980], interpolated with [*Lee et al*., 2015] between 325 and 345 nm; (2) 350-550 nm from [*Lee et al*., 2015]; (3) [*Pope and Fry*, 1997] for 555-725 nm; (4) [*Hale and Querry*, 1973], table 1, for 725-900 nm (the latter with 25 nm increments so linearly interpolated to 5 nm values]. Numbers provided as extinction coefficients k_W are to be converted using $\alpha_W(\lambda) = 4\pi k_W/\lambda$, where wavelengths are in [m] for extinctions in [m^{-1}].

The Chlorophyll absorption $\alpha_{ph}(\lambda)$ is given by two regimes. The first regime applies to the range 300-400 nm, and relies on linear interpolation of two sets of coefficients $\{a_1(\lambda), b_1(\lambda)\}$ at 10 nm intervals in this range [*Vasilkov et al*., 2005]. The absorption is given by:

$$\alpha_{Ph}(\lambda, C) = C a_1(\lambda) C^{-b_1(\lambda)}, \quad \text{(A4.1.1)}$$

where C is the pigment concentration (input value). Below 300 nm, there is no extrapolation - the value at 300 nm is used beyond the lower end of this range. The second regime applies to the range 400-720 nm, and relies on linear interpolation of two sets of coefficients $\{a_2(\lambda), b_2(\lambda)\}$ at 10 nm intervals [*Lee et al*., 2005]. The absorption is given by:

$$\alpha_{Ph}(\lambda, C) = [a_2(\lambda) + b_2(\lambda)\ln(a_{440})]a_{440}, \quad \text{(A4.1.2)}$$

where $a_{440} = 0.06C^{0.65}$, the well-known formula from [*Morel and Maritorena*, 2001]. Above 720 nm, there is no extrapolation - the value at 720 nm is used beyond this range.

The CDOM absorption is given by [*Morel and Gentili*, 2009], where λ is in nm:

$$\alpha_{CDOM}(\lambda, C) = 0.0524C^{0.63}exp[-0.018(\lambda - 412)]. \quad \text{(A4.1.3)}$$

The complete absorption is then

$$\alpha_{TOT}(\lambda, C) = \alpha_W(\lambda) + \alpha_{ph}(\lambda, C) + \alpha_{CDOM}(\lambda, C). \quad \text{(A4.1.4)}$$

For water scattering coefficients we use a formula from [*Zhang et al.*, 2009]:

$$b_W(\lambda) = 0.0026\left(\frac{0.42}{\lambda}\right)^{4.3}. \quad \text{(A4.1.5)}$$

For pigment scattering, we use the following from [*Morel and Maritorena*, 2001]:

$$b_{Ph}(\lambda, C) = b_{Pb}(C)\beta_{bbp}(C, \lambda); \quad \text{(A4.1.6)}$$

$$b_{Pb}(C) = 0.416C^{0.766};\ \beta_{bbp}(C, \lambda) = 0.002 + 0.01[0.5 - 0.25\log_{10} C]\left(\frac{\lambda}{0.55}\right)^{V},$$

where the exponent $V = 0$ for $C > 2$, and $V = 0.5[\log_{10} C - 0.3]$ for $C \le 2$. The complete scattering is then

$$b_{TOT}(\lambda, C) = b_W(\lambda) + b_{ph}(\lambda, C). \quad \text{(A4.1.7)}$$

VLIDORT Version 2.6 formulation.

In the original formulation for Version 2.6 of VLIDORT, the following formula was used to get the basic ocean-surface reflectance [*Morel and Gentili*, 1992]:

$$R(C, \lambda, \mu_0) = f(\mu_0) R_{TOT}(\lambda, C) \equiv f(\mu_0) \frac{b_{TOT}(\lambda, C)}{a_{TOT}(\lambda, C)}; \quad \text{(A4.1.8)}$$

$$f(\lambda, C, \theta_0) = d_0 - d_1\eta - d_2\eta^2 + (d_3\eta - d_4)\mu_0; \qquad \eta = \frac{b_W(\lambda)}{b_{TOT}(\lambda, C)}. \quad \text{(A4.1.9)}$$

Here, $f(\lambda, C, \theta_0)$ is given with 5 constants $\{d_0, d_1, d_2, d_3, d_4\}$ ={0.6279, 0.0227, 0.0513, 0.2465, 0.3119}, and $\mu_0 = \cos\theta_0$.

In order to assign the water-leaving radiance, develop the complete reflectance term:

$$R'(C, \lambda, \mu_0) = \frac{R(C, \lambda, \mu_0)}{1 - \omega R(C, \lambda, \mu_0)}. \quad \text{(A4.1.10)}$$

Here, albedo $\omega = 0.485$. The isotropic water-leaving radiance is then obtained after passage through the air-ocean interface:

$$S_{iso}(C, \lambda, \mu_0) \approx \frac{\mu_0}{\pi} T(\theta_0) \frac{R'(C, \lambda, \mu_0)}{|n_w|^2}. \quad \text{(A4.1.11)}$$

For the flat surface case, we assumed the interface transmittance $T(\theta_0) = 1$ (this is actually quite a good approximation), and n_w is the relative refractive index of water to air. For the rough surface case $T(\theta_0)$ may be computed using a glint-type calculation based on wind-speed and direction (not given here). Also for the rough surface case, we can define interface transmittances (from water to air) into the discrete ordinate and viewing directions - this is the non-isotropic case, which was not available in the flat-surface case for this formulation. See below for more details.

VLIDORT Version 2.8 formulation.

The above formulation takes no account of the atmospheric transmittance $T_{ATM}(\theta_0)$ at the surface which is propagated through the interface, and this has been remedied in the new scheme for LIDORT Version 3.8 and VLIDORT Version 2.8. In the previous formulation, the ratio $T_{ATM}(\theta_0)/Q$ was made implicit in the factor μ_0/π appearing the above equation.

Also, we replace the $f(\lambda, C, \theta_0)$ calculation with the direction-dependent ratio $\rho \equiv f/Q$ from [*Morel et al.*, 2002]. The isotropic water-leaving radiance is then:

$$S(C, \lambda, \theta_0, \gamma, \varphi) = T_{ATM}(\theta_0) T(\theta_0) \frac{R^*(C, \lambda, \theta_0, \gamma, \varphi)}{|n_w|^2}, \quad \text{(A4.1.12)}$$

$$R^*(C, \lambda, \theta_0, \gamma, \varphi) = \frac{\rho(C, \lambda, \theta_0, \gamma, \varphi) R_{TOT}(\lambda, C)}{1 - \omega f(C, \lambda, \theta_0) R_{TOT}(\lambda, C)}; \quad \text{(A4.1.13)}$$

Here, the "f/Q" quantity $\rho(C, \lambda, \theta_0, \gamma, \varphi)$ is a function of wavelength, pigment concentration, solar zenith angle, outgoing zenith angle γ and relative azimuth φ, and we use a tabulated form of this function provided by David Antoine (private communication).

The quantity $\bar{\rho}(C, \lambda, \theta_0)$ is obtained from this table by averaging over all viewing and azimuth angles, then interpolating with wavelength λ (linearly), with the logarithm $\ln C$ of the pigment concentration (by cubic-spline interpolation – necessary because we want smooth and continuous

derivatives with respect to C when considering linearized output) and against the cosine of the solar angle μ_0 (linearly). This quantity then defines the "isotropic" water-leaving contribution:

$$S_{iso}(C,\lambda,\theta_0) = T_{ATM}(\theta_0)T(\theta_0)\frac{\bar{R}^*(C,\lambda,\theta_0)}{|n_w|^2}; \quad \text{(A4.1.14)}$$

$$\bar{R}^*(C,\lambda,\theta_0) = \frac{\bar{\rho}(C,\lambda,\theta_0)R_{TOT}(\lambda,C)}{1-\omega f(C,\lambda,\theta_0)R_{TOT}(\lambda,C)}. \quad \text{(A4.1.15)}$$

The azimuth dependence is very weak in these "f/Q" tables, and at the time of writing, we have omitted this dependence in the surface leaving for the present formulation. However, we can derive non-isotropic surface-leaving "f/Q" values by interpolating table entries with the cosine of the outgoing angle - the resulting table extractions are $\tilde{\rho}_v(C,\lambda,\theta_0,\gamma_v)$ and $\tilde{\rho}_d(C,\lambda,\theta_0,\mu_d)$ for each viewing angle γ_v and discrete ordinate stream μ_d; these quantities are azimuth-averaged only. We then have:

$$S_v(C,\lambda,\theta_0,\gamma_v) = T_{ATM}(\theta_0)T(\theta_0)\frac{R_v^*(C,\lambda,\theta_0,\gamma_v)}{|n_w|^2}; \quad \text{(A4.1.16)}$$

$$R_v^*(C,\lambda,\theta_0,\gamma_v) = \frac{\tilde{\rho}_v(C,\lambda,\theta_0,\gamma_v)R_{TOT}(\lambda,C)}{1-\omega f(C,\lambda,\theta_0)R_{TOT}(\lambda,C)}, \quad \text{(A4.1.17)}$$

and similarly for the discrete ordinate directions.

It remains to determine the flux transmittance $T_{ATM}(\theta_0)$. One of the basic issues here is that this quantity is defined in terms of atmospheric radiative transfer - it is obtained by calculating the total atmospheric direct and diffuse downwelling flux at the surface. This is of course complicates the separation between the SL supplement and the VLIDORT calculation to follow which is to be based on the supplement input; furthermore, $T_{ATM}(\theta_0)$ will in general depend on the surface leaving contribution and hence on ocean constituents.

In the first instance, we assume that this module treats the ocean surface as dark, in which case $T_{ATM}(\theta_0)$ has no dependence on ocean properties, and VLIDORT remains decoupled from VSLEAVE. We then drop the $T_{ATM}(\theta_0)$ term from the above VSLEAVE equations based on ocean optics, and only re-introduce this term once it is computed inside VLIDORT. The simplest approximation to this term is the expression noted in [*Gordon and Wang*, 1994]:

$$T_{ATM}(\theta_0) = \exp\left[-\tfrac{1}{2}\frac{\tau_{ATM}}{\mu_0}\right], \quad \text{(A4.1.18)}$$

where τ_{ATM} is the total optical depth of the whole atmosphere. This is very easy to implement in VLIDORT. As an alternative to this expression, we have developed a look-up table of $T_{ATM}(\theta_0)$ for a Rayleigh atmosphere over a dark surface; this was obtained by running VLIDORT in multiple-scatter mode for a 270-900 nm wavelength range, and a number of solar zenith angles from 0 to 88 degrees; this table accounts for solar beam attenuation in a curved atmosphere. The default adopted in the Version 2.8 VLIDORT code is to generate the Rayleigh-approximated $T_{ATM}(\theta_0)$ from the supplement as a diagnostic output, to be used in VLIDORT as desired.

In this simple situation where atmosphere and water-leaving radiance calculations are decoupled, it is still possible to define VLIDORT weighting functions with respect to pigment concentration, since only the VSLEAVE supplement will have this dependency, and the resulting Jacobians can be treated just like any other surface linearization.

Of course the simple formula or the use of a Rayleigh-based calculation is not an adequate substitute for more realistic situations with atmospheric aerosols present - ultimately one must use on-the-fly VLIDORT calculations. We address this point next.

A full calculation of $T_{ATM}(\theta_0)$ (regardless of whether the surface is dark or ocean) can only be made using the full multiple-scatter formalism. Indeed, this is a VLIDORT-within-VLIDORT simulation, for just one Fourier term, and with no post-processing, since we require only the downwelling flux at the surface. In order to obtain self-consistency ("coupling"), we adopt the following procedure. Start with a dark-surface first guess T_0 for the flux transmittance, using the simple expression in Eq. (A4.1.18). Use this value T_0 to set the surface-leaving input, and then do a full calculation to establish a new flux transmittance T_1 at the surface. Repeat the process, now using T_1 to set the surface-leaving term and thereby obtaining a new value T_2. This process is iterated until the relative differences in T-values are less that some small-number criterion. In practice, convergence is achieved rapidly after only a few iterations. This module is somewhat time-consuming (after all, we are doing a full Fourier-zero MS-field computation at each iteration step). In VLIDORT, use of this iterative procedure is controlled by a Boolean flag (DO_TF_ITERATION), and two simple controls (DO_TF_MAXITER, and DO_TF_ CRITERION); see Table A in section 5.4 of the Main Guide.

Linearization. Here we are interested in Jacobians with respect to the pigment concentration C. Differentiation of the above semi-empirical formulas is straightforward. Starting with the chlorophyll absorption, we find

$$\dot{\alpha}_{Ph}(\lambda, C) \equiv \frac{\partial \alpha_{Ph}(\lambda,C)}{\partial C} = \alpha_{Ph}(\lambda, C)\frac{[1-b_1(\lambda)]}{C}; \qquad \text{(A4.1.19)}$$

$$\dot{\alpha}_{Ph}(\lambda, C) \equiv \frac{\partial \alpha_{Ph}(\lambda,C)}{\partial C} = \frac{0.65}{C}[\alpha_{Ph}(\lambda, C) + b_2(\lambda)a_{440}], \qquad \text{(A4.1.20)}$$

for the two absorption regimes. Similar considerations apply to the derivatives $\dot{b}_{ph}(\lambda, C)$ of the scattering coefficient. From these starting points, one can apply chain-rule differentiation to get

$$\frac{\partial f(\mu_0)}{\partial C} = [-d_1 - 2\eta d_2 + \mu_0 d_3]\frac{\partial \eta}{\partial C}; \qquad \frac{\partial \eta}{\partial C} = -\frac{\eta \dot{b}_{ph}(\lambda,C)}{b_{TOT}(\lambda,C)}; \qquad \text{(A4.1.21)}$$

$$\frac{\partial R(C,\lambda,\mu_0)}{\partial C} = \frac{\partial f(\mu_0)}{\partial C}R_{TOT}(\lambda, C) + f(\mu_0)\frac{\dot{b}_{ph}(\lambda,C) - \dot{\alpha}_{Ph}(\lambda,C)R_{TOT}(\lambda,C)}{a_{TOT}(\lambda,C)}. \qquad \text{(A4.1.22)}$$

$$\frac{\partial R'(C,\lambda,\mu_0)}{\partial C} = \frac{\partial R(C,\lambda,\mu_0)}{\partial C}\frac{1-\omega}{1-\omega R(C,\lambda,\mu_0)}. \qquad \text{(A4.1.23)}$$

These three results apply to the Version 2.6 formulation. For the Version 2.8 formalism, the additional quantities are the table-interpolated "foQ" ratios $\bar{\rho}(C, \lambda, \theta_0)$, $\tilde{\rho}_v(C, \lambda, \theta_0, \gamma_v)$ and $\tilde{\rho}_d(C, \lambda, \theta_0, \mu_d)$. Since the interpolation with $\ln C$ is done by splines, it is easy to differentiate with respect to this variable during the interpolation process.

We note that, when the flux transmittance $T_{ATM}(\theta_0)$ is calculated for a dark surface, and thus has no dependence on the pigment concentration; it plays no part in this linearization. *Linearization for the iterative procedure wherein the atmosphere and ocean are coupled self-consistently through the flux transmittance is not currently enabled*.

An application of this new water-leaving model may be found in [*Vasilkov et al*., 2017].

Rough Surface. This option was developed for the Version 2.7 formulation. The above analysis for the ocean reflectance still holds, but the rough surface option allows us to generate glitter-dependent transmission terms through the water-air interface, both for the incoming solar directions $\vec{T}_{aw}(\theta_0)$, and for outgoing line-of-sight $\overleftarrow{T}_{wa}(\theta_0, \gamma_v)$ and discrete-ordinate $\overleftarrow{T}_{wa}(\theta_0, \mu_d)$ directions respectively. Thus for instance, the rough surface water-leaving term for a viewing angle is

$$S_{v,RS}(C, \lambda, \theta_0, \gamma_v) = \vec{T}_{aw}(\theta_0) S_v(C, \lambda, \theta_0, \gamma_v)\, \overleftarrow{T}_{wa}(\theta_0, \gamma_v), \qquad \text{(A4.1.24)}$$

in terms of the previously derived value.

A5. Adjunct References

Anderson, E., Z. Bai, C. Bischof, J. Demmel, J. Dongarra, J. Du Croz, A. Greenbaum, S. Hammarling, A. McKenney, S. Ostrouchov, and D. Sorensen, LAPACK User's Guide, 2nd Edition, Philadelphia, SIAM (Society for Industrial and Applied Mathematics), 1995.

Bhartia, P. K., Algorithm Theoretical Baseline Document, TOMS v8 Total ozone algorithm, (http://toms.gsfc.nasa.gov/version8/version8/update.html), 2003.

Caudill, T. R., D. E. Flittner, B. M. Herman, O. Torres, and R. D. McPeters, Evaluation of the pseudo-spherical approximation for backscattered ultraviolet radiances and ozone retrieval. *J. Geophys. Res.*, **102**, 3881-3890, 1997.

Chandrasekhar, S., Radiative Transfer, Dover Publications Inc., New York, 1960.

Cox, C., and W. Munk, Statistics of the sea surface derived from sun glitter. *J. Mar. Res*., **13,** 198-227, 1954.

Dahlback, A., and K. Stamnes, A new spherical model for computing the radiation field available for photolysis and heating at twilight. *Planet. Space Sci.*, **39**, 671, 1991.

de Rooij, W. A., and C. C. A. H. van der Stap Expansion of Mie scattering matrices in generalized spherical functions. *Astron. Astrophys.*, **131**, 237-248, 1984.

EPS/METOP System – Single Space Segment – GOME-2 requirements Specification. ESA/EUMETSAT, MO-RS-ESA-GO-0071, 1999: Issue 2.

Gordon HR, Wang M. Retrieval of water-leaving radiance and aerosol optical thickness over the oceans with SeaWiFS: A preliminary algorithm. *Applied Optics*, **33**; 443-452, 1994.

Hale, G. M., and M. R. Querry. Optical constants of water in the 200-nm to 200-um wavelength region. *Applied Optics*, **12** (3), 555{563, doi:10.1364/AO.12.000555, 1973.

Hovenier, J. W., C. van der Mee, and H. Domke, Transfer of Polarized Light in Planetary Atmospheres Basic Concepts and Practical Methods, Kluwer, Dordrecht, 2004.

Jin, Z., T. Charlock, K. Rutledge, K. Stamnes, and Y. Wang, Analytic solution of radiative transfer in the coupled atmosphere-ocean system with a rough surface. *Applied Optics*, **45**, 7433-7455, 2006.

Kotchenova S. Y., E. F. Vermote, R. Matarrese, and F. J. Klemm. Validation of a vector version of the 6S radiative transfer code for atmospheric correction of satellite data. Part I: Path radiance. *Applied Optics*, **45**, 6762-74, 2006.

Lee, Z. P., K. P. Du, and R. Arnone. A model for the diffuse attenuation coefficient of downwelling irradiance. *J. Geophys. Res*. **110** (C02016). http://dx.doi.org/10.1029/2004JC002275, 2005.

Lee, Z., J. Wei, K. Voss, M. Lewis, A. Bricaud, and Y. Huot. Hyperspectral absorption coefficient of "pure" seawater in the range of 350-550 nm inverted from remote sensing reflectance. *Applied Opt*ics, **54**, 546-558, doi:10.1364/AO.54.000546, 2015.

Levelt, P. F., G. H. J. van den Oord, M. R. Dobber, A. Mälkki, J. de Vries, P. Stammes, J. O. V. Lundell, and H. Saari, The Ozone Monitoring Instrument. *IEEE Transact Geoscience Remote Sensing*, **44**, 1093-1101, 2006.

Mackowski, D. W., and M. I. Mishchenko, Calculation of the T matrix and the scattering matrix for ensembles of spheres. *J. Opt. Soc. Am. A*, **13**, 2266-2278, 1996.

Maignan, F., F.-M. Bréon, E. Fédèle, and M. Bouvier, Polarized reflectance of natural surfaces: Spaceborne measurements and analytical modeling. *Rem. Sens Env.*, **113**, 2642-2650, 2009.

Mishchenko, M. I., and L. D. Travis, Satellite retrieval of aerosol properties over the ocean using polarization as well as intensity of reflected sunlight. *J. Geophys. Res.*, **102**, 16989, 1997.

Mishchenko, M. I., and L. D. Travis, Capabilities and limitations of a current FORTRAN implementation of the T-matrix method for randomly oriented, rotationally symmetric scatterers. *J. Quant. Spectrosc. Radiat. Transfer*, **60**, 309-324, 1998.

Mishchenko, M., J. Hovenier, and L. Travis, Eds., Light Scattering by non-Spherical Particles, Academic Press, San Diego, 2000.

Mishchenko, M. I., Microphysical approach to polarized radiative transfer: extension to the case of an external observation point. *Applied Optics*, **42**, 4963- 4967, 2003.

Mishchenko, M. I., B. Cairns, J. E. Hansen, L. D. Travis, R. Burg, Y. J. Kaufman, J. V. Martins, and E. P. Shettle, Monitoring of aerosol forcing of climate from space: Analysis of measurement requirements. *J. Quant. Spectrosc. Radiat. Transfer*, **88**, 149-161, 2004.

Mishchenko, M. I., L. D. Travis, and A. A. Lacis. Scattering, Absorption and Emission of Light by small particles. Cambridge University Press, Cambridge, U.K., 2006.

Morel, A., and B. Gentili. A simple band ratio technique to quantify the colored dissolved and detrital organic material from ocean color remotely sensed data. *Remote Sens. Env.*, **113**, 2009.

Morel, A., and S. Maritorena. Bio-optical properties of oceanic waters: A reappraisal. *J. Geophys Res*., **106**: 7163-7180, 2001.

Nadal, F., and F.-M Bréon, Parameterization of surface polarized reflectance derived from POLDER spaceborne measurements. IEEE *Trans. Geosci. Remote*, **37**, 1709–1718, 1999.

Nakajima, T., and M. Tanaka, Algorithms for radiative intensity calculations in moderately thick atmospheres using a truncation approximation. *J. Quant. Spectrosc. Radiat. Transfer*, **40**, 51-69, 1988.

Pope, R. M., and E. S. Fry. Absorption spectrum (380-700nm) of pure water. II. Integrating cavity measurements. *Applied Optics*; **36**: 8710-8723, 1997.

Quickenden, T. I., and J. A. Irvin. The ultraviolet absorption spectrum of liquid water. *J. Chem. Phys*., **72**(8):4416-4428, 1980.

Rozanov, A. V., V. V. Rozanov, and J. P. Burrows, Combined differential-integral approach for the radiation field computation in a spherical shell atmosphere: Non-limb geometry. *J. Geophys. Res.*, **105**, 22937-22942, 2000.

Sancer, M., Shadow-corrected electromagnetic scattering from a randomly-rough ocean surface. *IEEE Trans Antennas Propag.*, **AP-17**, 557-585, 1969.

Sayer, A. M., G. E. Thomas, and R. G. Grainger. A sea surface reflectance model for (A)ATSR, and application to aerosol retrievals. *Atmos. Meas. Tech*., **3**, 813–838, doi:10.5194/amt-3-813-2010, 2010.

Siewert, C. E., On the equation of transfer relevant to the scattering of polarized light. *Astrophysics J.*, **245**, 1080-1086, 1981.

Siewert, C. E., On the phase matrix basic to the scattering of polarized light. *Astron. Astrophys.*, **109**, 195-200, 1982.

Siewert, C. E., A discrete-ordinates solution for radiative transfer models that include polarization effects. *J. Quant. Spectrosc. Radiat. Transfer*, **64**, 227-254, 2000.

Spurr, R., T. Kurosu, and K. Chance, A linearized discrete ordinate radiative transfer model for atmospheric remote sensing retrieval. *J. Quant. Spectrosc. Radiat. Transfer*, **68**, 689–735, 2001.

Spurr, R., Simultaneous derivation of intensities and weighting functions in a general pseudo-spherical discrete ordinate radiative transfer treatment. *J. Quant. Spectrosc. Radiat. Transfer*, **75**, 129–175, 2002.

Spurr, R. J. D., LIDORT V2PLUS: A comprehensive radiative transfer package for UV/VIS/NIR nadir remote sensing; a General Quasi-Analytic Solution. *Proc. S.P.I.E. International Symposium, Remote Sensing 2003*, Barcelona, Spain, September 2003.

Spurr, R. J. D., A New Approach to the Retrieval of Surface Properties from Earthshine Measurements. *J. Quant. Spectrosc. Radiat. Transfer*, **83**, 15-46, 2004.

Spurr, R., LIDORT and VLIDORT: Linearized pseudo-spherical scalar and vector discrete ordinate radiative transfer models for use in remote sensing retrieval problems. *Light Scattering Reviews*, Volume 3, ed. A. Kokhanovsky, Springer, 2008.

Spurr, R, and M. Christi, On the generation of atmospheric property Jacobians from the (V)LIDORT linearized radiative transfer models. *J. Quant. Spectrosc. Radiat. Transfer*, DOI: 10.1016/j.jqsrt.2014.03.011, 2014.

Spurr, R, and M. Christi, The LIDORT and VLIDORT Linearized Scalar and Vector Discrete Ordinate Radiative Transfer Models: Updates in the last 10 Years. *Light Scattering Reviews*, Volume 12, ed. A. Kokhanovsky, Springer, 2019.

Stamnes, K., and P. Conklin, A new multi-layer discrete ordinate approach to radiative transfer in vertically inhomogeneous atmospheres. *J. Quant. Spectrosc. Radiat. Transfer*, **31**, 273, 1984.

Stamnes, K., S.-C. Tsay, W. Wiscombe, and K. Jayaweera, Numerically stable algorithm for discrete ordinate method radiative transfer in multiple scattering and emitting layered media. *Applied Optics*, **27**, 2502-2509, 1988.

Stamnes, K., S-C. Tsay, W. Wiscombe, and I. Laszlo, DISORT: A general purpose Fortran program for discrete-ordinate-method radiative transfer in scattering and emitting media. Documentation of Methodology Report, available from 82H82H83Hftp://climate.gsfc.nasa.gov/wiscombe/Multiple_scatt/, 2000.

Stammes, P., J. F. de Haan, and J. W. Hovenier, The polarized internal radiation field of a planetary atmosphere. *Astron. Astrophys*., **225**, 239-259, 1989.

Thomas, G. E., and K. Stamnes, Radiative Transfer in the Atmosphere and Ocean, Cambridge University Press, 1999.

Van Oss, R. F., and R. J. D. Spurr, Fast and accurate 4 and 6 stream linearized discrete ordinate radiative transfer models for ozone profile retrieval, *J. Quant. Spectrosc. Radiat. Transfer*, **75**, 177-220, 2002.

Vasilkov, A. P., J. R. Herman, Z. Ahmad, M. Karu, and B. G. Mitchell. Assessment of the ultraviolet radiation field in ocean waters from space-based measurements and full radiative-transfer calculations. *Appl. Opt*., **44** (14), 2863-2869, doi:812 10.1364/AO.44.002863, 2005.

Vasilkov, A. P., W. Qin, N. Krotkov, L. Lamsal, R. Spurr, D. Haffner, J. Joiner, E.-S. Yang, and S. Marchenko, Accounting for the effects of surface BRDF on satellite cloud and trace-gas retrievals: a new approach based on geometry-dependent Lambertian equivalent reflectivity applied to OMI algorithms. *Atmos. Meas. Tech*., **10**, 333–349, doi:10.5194/amt-10-333-2017, 2017.

Vermote, E. F., D. Tanré, J. L. Deuzé, M. Herman, and J. J. Morcrette. Second simulation of the satellite signal in the solar spectrum, 6S: an overview. IEEE *Trans. Geosci. Remote Sens*., **35**, 675– 686, 1997.

Vestrucci, M., and C. E. Siewert, A numerical evaluation of an analytical representation of the components in a Fourier decomposition of the phase matrix for the scattering of polarized light. *J. Quant. Spectrosc. Radiat. Transfer*, **31,** 177-183, 1984.

Wanner, W., X. Li, and A. Strahler, On the derivation of kernels for kernel-driven models of bidirectional reflectance. *J. Geophys. Res.*, **100**, 21077, 1995.

Wellemeyer, C., S. L. Taylor, C. J. Seftor, R. D. McPeters and P. K. Bhartia, A correction for total ozone mapping spectrometer profile shape errors at high latitude. *J. Geophys. Res.*, **102**, 9029-9038, 1997.

Zhang, X., L. Hu, and M.-X. He. Scattering by pure seawater: Effect of salinity. *Opt. Express*., **17**, 5698{5710, doi:10.1364/OE.17.005698, 2009.